

Title page

Light spectra trigger divergent gene expression in barley cultivars

Arantxa Monteagudo ^{a*}, Álvaro Rodríguez del Río ^{a,1*}, Bruno Contreras-Moreira ^{a,b,2}, Tibor Kiss ^{c,3}, Marianna Mayer ^c, Ildikó Karsai ^c, Ernesto Igartua ^a, Ana M. Casas ^{a#}

^a Aula Dei Experimental Station (EEAD-CSIC), Avda. Montañana 1005, E-50059 Zaragoza, Spain

^b Fundación ARAID, Zaragoza, Spain

^c Centre for Agriculture Research ELKH (ATK), H-2462 Martonvásár, Hungary.

* These authors contributed equally to this work

Corresponding author: acasas@eead.csic.es

Arantxa Monteagudo: amonteagudo@eead.csic.es

Álvaro Rodríguez del Río: alvarordr94@gmail.com

Bruno Contreras-Moreira: bcontreras@ebi.ac.uk

Tibor Kiss: kiss.tibor@atk.hu

Marianna Mayer: mayer.marianna@agrar.mta.hu

Ildikó Karsai: karsai.ildiko@agrar.mta.hu

Ernesto Igartua: igartua@eead.csic.es

Ana M. Casas (corresponding author): acasas@eead.csic.es.

Date of submission: 3-February-2021

Number of tables and figures: 1 table, 9 figures.

Word count: 5277

Running title: Light spectra affects barley gene expression

¹ Present address: Center for Plant Biotechnology and Genomics, National Institute of Agricultural and Food Research and Technology (INIA-UPM), Pozuelo de Alarcón, Spain

² Present address: The European Bioinformatics Institute (EMBL-EBI), Wellcome Trust Genome Campus, Hinxton, United Kingdom

³ Present address: Food and Wine Research Institute, Eszterházy Károly University, Eger, Hungary

Highlight

Development genes were affected by light quality in the barley varieties tested. Different grades of sensitivity were related to the expression of transcription factors, senescence, light signaling and cold-regulated genes.

1 **Abstract**

2 Light spectra influence barley development, causing a diverse range of responses among
3 cultivars that are poorly understood. Here, we exposed three barley genotypes with
4 different light sensitivities to two light sources: fluorescent bulbs, over-representing green
5 and red wavebands, and metal halide lamps, with a more balanced spectrum. We used RNA
6 sequencing to identify the main genes and pathways involved in the different responses,
7 and RT-qPCR to validate the expression values. Different grades of sensitivity to light
8 spectra were associated with transcriptional reprogramming, plastid signals, and
9 photosynthesis. The genotypes were especially divergent in the expression of genes
10 regulated by transcription factors from MADS-box, WRKY, and NAC families, and in
11 specific photoreceptors such as phytochromes and cryptochromes. Variations in light
12 spectra also affected the expression of circadian clock, flowering time, and frost tolerance
13 genes, among others, resembling plant responses to temperature. The relation between
14 *PPD-H1*, *HvVRN1*, and *HvFT1* expression might explain genotypic differences. Light-
15 sensitive genotypes experienced a partial reversion of the vernalization process and
16 senescence-related stress under the less favorable light quality conditions. The observed
17 light-quality sensitivities reveal a complex mechanism of adaptation to regions with
18 specific light quality features and/or possible regulation of light spectra in plant
19 development during early spring.

20 **Keywords**

21 Barley, cold-regulated genes, development, light quality, RNA-seq, senescence, signaling,
22 transcription factors.

23

24 **Abbreviations**

25 DE, differentially expressed; DEV, developmental stage; F, fluorescent; LD, long day; M,

26 metal halide; TF, transcription factor.

27

28 **Introduction**

29 As sessile organisms, plants have evolved adapting and surviving in a wide variety of
30 environments. One of the main developmental triggers is light, whose features regulate
31 growth and determine the adaptation to changing environments with different light
32 duration, quantity, and quality (Franklin, 2009; Ugarte *et al.*, 2010).

33 Like day length, light quality and intensity are not constant in natural environments, as
34 revealed by the different spectra that occur in different moments of the day, seasons,
35 climates, and atmospheric conditions (Holmes and Smith, 1977; Smith, 1982). Although
36 the responses of plants to some light features have been thoroughly analyzed (Franklin,
37 2009; Ugarte *et al.*, 2010; Monostori *et al.*, 2018), there is a gap in the study of natural
38 genetic variation in crop plants and its possible effect on crop development and adaptation.
39 For instance, light quality effects have been widely studied in *Arabidopsis* (Adams *et al.*,
40 2009), but only to a lesser extent in cereals (Ugarte *et al.*, 2010).

41 Differential regulation of genes whose expression levels are affected by light quality signals
42 may reflect different abilities to compete in diverse species or crop varieties. The
43 concentration and efficiency of photoreceptors that control the dynamics of red/far-red
44 (R/FR) light signaling are highly variable in different species and crop varieties (Merotto Jr.
45 *et al.*, 2009). Higher plants possess two types of signal-transducing photoreceptors:
46 phytochromes (in cereals PhyA, PhyB, and PhyC) absorbing principally in the 600-800 nm
47 waveband, and cryptochromes (Cry1, Cry2), absorbing only in the 300-500 nm band
48 (Smith 1982; Casal 1993). Phytochrome proteins are characterized by a red/far-red
49 photochromicity, changing their spectral absorbance properties upon light absorption. Their

50 biologically inactive form activates after absorbing R light and reverts to inactive after
51 absorbing FR light (Rockwell *et al.*, 2006). As dimeric proteins, the role of homo and
52 heterodimers is still an open area of research but it has been proven that both *PhyB* and
53 *PhyC* genes are required for the induction of wheat flowering under long photoperiods
54 (Pearce *et al.*, 2016). Cryptochromes have been found to regulate photomorphogenesis and
55 the expression of genes involved in blue light signaling and stress response (Kleine *et al.*
56 2007). Both phytochrome dimers and cryptochromes interact with transcription factors (TF)
57 known as Phytochrome Interacting Factors (PIFs) (Leivar and Monte, 2014; Pedmale *et al.*,
58 2016), regulating clock and flowering time genes (Oakenfull & Davis 2017), and are at the
59 top of fundamental light-driven processes.

60 Together with light, crops responses to temperature are receiving increasing attention, and
61 more efforts are being dedicated to unraveling the catalog of cross-talk and nodes at which
62 both signals converge (Franklin *et al.*, 2014). Both are particularly important in winter
63 cereals, which need to satisfy cold needs (called *vernalization*) before the spring when long
64 days (LD) mark the signal to flower. Thus, perception of photoperiod and cold are critical
65 to enabling flowering timely. Two main genes control the vernalization response in winter
66 cereals. In barley, these genes are *HvVRN1*, an *API*-like MADS-box TF, and promoter of
67 flowering, and *HvVRN2*, also known as *ZCCT-Ha-c*, a zinc-finger and CCT domain-
68 containing repressor protein that belongs to the *CONSTANS*-like family (Trevaskis *et al.*,
69 2003; Yan *et al.*, 2004). Both interact with the floral pathway integrator *HvFT1* (Yan *et al.*,
70 2006). When the cold requirement has not been satisfied, long-days promote *HvVRN2*
71 expression, repressing *HvFT1*, and delaying flowering until plants complete vernalization
72 (Trevaskis *et al.*, 2006; Hemming *et al.*, 2008). In temperate cereals, other members of the

73 MADS-box TF family genes, such as the *Flowering Locus C* (FLC)-clade member *OS2*
74 (*ODDSOC2*) and the *Short Vegetative Phase* (SVP)-clade member, *VRT2*, cause a delay
75 until experiencing enough cold (Kane *et al.*, 2005; Greenup *et al.*, 2010; Xie *et al.*, 2019).
76 Cold induces *HvVRN1*, which then represses *HvVRN2*, and together with the influence of
77 LD, allows the expression of the flowering integrator *HvFT1*. During the vernalization of
78 winter genotypes, the expression of the SVP-clade MADS-box TFs (*HvVRT2*, *HvBM1*, or
79 *HvBM10*) is up-regulated during the vegetative phase (Trevaskis *et al.*, 2007). Particularly,
80 *VRT2* participates in regulating the vernalization flowering pathway, interacting and
81 cooperating with *VRN1* (Xie *et al.*, 2019), and after the transition to the reproductive phase,
82 its expression declines (Kane *et al.*, 2005). The connection between photoreceptor and
83 photoperiod pathways has been attributed to *PhyC*, which activates the long-day
84 photoperiod response gene, *PPD-1* in LD (Nishida *et al.*, 2013; Chen *et al.*, 2014; Pankin *et*
85 *al.*, 2014; Woods *et al.*, 2014). Both *PhyC* and *PhyB* promote flowering under LD,
86 although *PhyB* regulates more genes than *PhyC* (Kippes *et al.*, 2020), particularly those
87 involved in vegetative development, hormone biosynthesis, and signaling, shade avoidance
88 response, abiotic stress tolerance (Pearce *et al.*, 2016), and cold tolerance (Franklin and
89 Quail, 2010; Novák *et al.*, 2016).

90 Motivated by the lack of studies on natural genetic variation in crop plants and its possible
91 effect on crop development and adaptation, we explored the phenotypic variability for plant
92 growth, in response to different light quality environments, in barley (*Hordeum vulgare*,
93 L.). Plants were exposed to two light sources: fluorescent light, which presents high peaks
94 at the 550-650 nm regions, corresponding to green and red wavebands, and metal halide
95 bulbs, which yield a more balanced spectrum. Although all genotypes had been vernalized

96 before the start of the experiment and temperature, photoperiod and light intensity were
97 identical and inductive to promote flowering, plants grown under fluorescent light showed
98 delayed development compared to those under metal halide light (Monteagudo *et al.* 2020).
99 We thus observed an effect of light quality on the expression of flowering time genes,
100 opening new questions about the regulation of photoperiod and vernalization pathways in
101 different barley varieties.

102 Here, we exposed three of the previously assessed genotypes to the same two contrasting
103 light spectral conditions to further investigate their gene expression patterns: an insensitive
104 line (minor response to light quality), Esterel, and two sensitive lines (major growth
105 differences between light quality conditions), Price (sensitive-intermediate) and WA1614-
106 95 (sensitive-extreme). The aims of this study were: a) to identify genes that explain the
107 different sensitivities of barley lines to light spectral quality, and b) to gain further
108 knowledge on the influence of light quality on development and on the expression of
109 flowering time genes. Here we provide evidence of the molecular mechanisms affected by
110 light quality. We identified key flowering pathway regulators, and other important genes
111 involved in development whose expression was affected in all varieties. Genotypic
112 differences in the expression of light signaling and cold responses were also found, which
113 might be related to barley adaptability to a wide range of environments and to an additional
114 regulation mechanism of plant development during early spring.

115 **Materials and Methods**

116 Plant material and phenotyping

117 We selected varieties Esterel, Price, and WA1614-95 (Supplementary Table S1), from a set
118 of 11 winter or facultative barley varieties described in a previous study (Monteagudo *et*
119 *al.*, 2020) that revealed different responses to light environments (see Figure 1).

120 The experiment was carried out at the phytotron facilities of the Agricultural Research
121 Institute of the Hungarian Academy of Sciences, Martonvásár (Hungary), using Conviron
122 PGR-15 growth chambers (Conviron Ltd., Canada). Two light treatments were established
123 in independent growth chambers. Two lamp types were used: Sylvania cool white
124 fluorescent (F) and Tungsram HGL-400 metal halide (M) light bulbs. The height of the
125 lamps in the F chamber was adjusted once per week to 1.4 m above the canopy, to match
126 the light intensity of the M chamber, in which the lights were set at a fixed height. The
127 conditions in both chambers were set to long photoperiod (16 h light/8h night), and $18 \pm$
128 1°C constant temperature, and light intensity of $250 \mu\text{mol m}^{-2} \text{s}^{-1}$. Temperature was
129 continuously monitored through an air-sampling channel, located in the middle of the
130 cabinet at canopy level. This system of temperature control eliminated the possibility that
131 plants experienced different temperatures at both chambers.

132 For phenotypic measurements, four seeds per genotype and treatment were sown in
133 individual pots (12 x 18 cm, 1.5 kg). Additionally, 20 seeds per genotype and treatment,
134 sown in groups of 5 plants/pot, were used for destructive samplings to record apex
135 development stage, and for gene expression studies. All plants were fully vernalized ($5 \pm$
136 2°C for 52 days under 8h light/16 h night, low-intensity metal-halide light bulbs) before

137 entering the light quality chambers, to synchronize the development of the three genotypes.
138 Plant development was monitored twice a week, checking for first node appearance (plant
139 developmental stage 31, or DEV31) and appearance of the awns just visible above the last
140 leaf sheath (DEV49). All these data were defined based on stages of the Zadoks's scale
141 (Zadoks *et al.*, 1974), following the description of Tottman *et al.* (1979). Apex dissection
142 was carried out 23 days after the end of the vernalization period in 3 plants per variety and
143 treatment. Phenotyping consisted of recording apex stage following the Waddington's scale
144 (Waddington *et al.*, 1983). Plants were grown to full maturity.

145 RNA extraction and transcriptome sequencing

146 Three genotypes were used for transcriptome analysis. Three biological replicates per
147 genotype and treatment were produced. Each biological replicate pooled the last expanded
148 leaves of the main tillers from two different plants. Leaves were sampled in the middle of
149 the light cycle, 20 days after the end of the vernalization period, and immediately frozen in
150 liquid N₂. Leaf samples for Real-time PCR quantification (qRT-PCR) validation were
151 obtained in an independent experiment, as reported by Monteagudo *et al.* (2020).

152 Total RNA was isolated with TRIzol (Thermo Fisher Scientific, Ltd.) followed by the
153 Qiagen RNeasy plant mini kit, following the manufacturer's instructions (Qiagen, Ltd.).
154 Then, the material was extracted in the QIAcube equipment (Qiagen, Ltd.) with an extra
155 step of DNase treatment programmed. RNA quality was assessed with a NanoDrop 2000
156 spectrophotometer (Thermo Fisher Scientific, Ltd.) at ATK (Hungary).

157 RNAseq was performed by Novogene (HK) Co. Ltd. (China) after quality controls by
158 agarose gel electrophoresis and Bioanalyzer 2100 (Agilent, USA; RIN \geq 6.3). Library

159 construction was developed from enriched RNA, using oligo(dT) beads. Then, mRNA was
160 randomly fragmented, followed by cDNA synthesis using random hexamers and reverse
161 transcriptase. After the first-strand synthesis, a custom second-strand synthesis buffer
162 (Illumina, USA) was added, with dNTPs, RNase H, and *Escherichia coli* polymerase F to
163 generate the second strand by nick-translation, and AMPure XP beads were used to purify
164 the cDNA. The final cDNA library was ready after a round of purification, terminal repair,
165 A-tailing, ligation of sequencing adapters, size selection, and PCR enrichment. Library
166 concentration was first quantified using a Qubit 2.0 fluorometer (Life Technologies) and
167 then diluted to 1 ng/μl before checking insert size on an Agilent 2100 and quantifying to
168 greater accuracy by quantitative PCR (library activity > 2 nM). Eighteen barcoded libraries
169 were multiplexed and sequenced, 2x150 bp paired-end reads, in an Illumina HiSeq™ 2500
170 sequencer, yielding on average 50 Million reads per sample. The whole dataset consisted of
171 18 samples, i.e. 3 biological replicates, from 3 varieties and 2 light conditions.

172 Raw reads were processed with Illumina CASAVA v1.8 (Illumina, USA). Low-quality
173 reads (reads with more than 50% low-quality base ($Q \leq 20$)) were removed. Reads from the
174 three genotypes were jointly assembled *de novo*, with the software Trinity (Haas *et al.*,
175 2013) (Figure 2). The obtained assembled transcripts had a median length of 366 bp. Raw
176 transcripts of all three genotypes were combined, followed by a step of hierarchical
177 clustering. Then, the longest transcripts were kept and unigenes were called with Corset
178 v1.05 (-m 10 to remove redundancy, Davidson and Oshlack, 2014). The median unigene
179 length was 779 bp. Raw reads of the sequencing experiments (accessions ERR3763262-
180 ERR3763279) and assembled *de novo* transcripts (ERZ1264422) have been submitted to
181 the European Nucleotide Archive.

182 Quantification of gene expression and differential expression analysis

183 There are several barley assembly references available. We tested eight references and
184 chose the most suitable for each purpose (Supplementary Information). We mapped clean
185 reads against each reference and quantified transcript abundance as Transcripts Per Million
186 (TPM) using Kallisto (Bray *et al.*, 2016). We used the R functions ‘heatmap’ and ‘hclust’
187 (R Core Team, 2020), to cluster the gene expression patterns from the experimental
188 replicates, from the three genotypes, under the two light conditions. The resulting clusters
189 were used to assess the expression quantification with several mapping references (see
190 Supplementary Information). The gene sets which grouped more biological replicates
191 together were selected for gene expression quantification. The barley reference genome
192 from cultivar Morex (named “**Morex CDS sequences**”) (Mascher *et al.*, 2017) was used
193 for all downstream analyses except GO enrichment, as these sequences lacked relevant GO
194 terms related to light responses. For this reason, assembled Zangqing320 PacBio reads,
195 from here on noted as “**Tibetan transcripts**” (Dai *et al.*, 2018), and the assembly
196 generated in this work (“**de novo assembly**”), were chosen for conducting the GO
197 enrichment analysis (Figure 2).

198 For ensuring the quality of the biological replicates, we calculated Pearson correlation
199 coefficients across the transcript abundance of biological samples and replicates derived
200 from reads mapped to “**Morex CDS sequences**”, with the R package “corrplot” (Wei and
201 Simko, 2017). Independently validated RNA-seq expression values were obtained through
202 qRT-PCR (ABI 7500, Applied Biosystems), performed on biological replicates for the
203 same varieties and conditions, grown in an independent experiment. Expression values of
204 10 genes (Supplementary Table S2) were calculated relative to *Actin*

205 (*HORVU5Hr1G039850.3*), taking into account the efficiency of each pair of primers. Each
206 PCR reaction contained 5 μ l of PowerUp SYBR Green Master Mix (Applied Biosystems),
207 0.5 μ M of each primer, and 250 ng of cDNA in a volume of 10 μ l. Reactions were run with
208 the following conditions: 2 min activation at 50°C, 10 min of pre-denaturation at 95°C;
209 followed by 44 cycles of 15 s denaturation at 95°C, 50 s annealing at 60°C, and 45 s of
210 extension step at 72°C, ending with a melting curve 60°–95°C default ramp rate. The same
211 normalization (relative to *Actin*) was accomplished for the number of TPM values and
212 compared for the same genes and treatments in the RNA-seq. This procedure was carried
213 out with a total of 60 points (average of 3 biological replicates per treatment and variety, in
214 10 genes).

215 We used Sleuth (Pimentel *et al.*, 2017) for calculating differential expression (DE) of the
216 genes from the three barley varieties. Nine DE analyses (M vs F for each one of three
217 genotypes, and comparisons between pairs of genotypes for each light quality condition)
218 were achieved for each mapping reference. However, here we only report results on the DE
219 genes calculated from the three aforementioned references (Figure 2 and Supplementary
220 Information). We validated the Kallisto/Sleuth methodology by comparing it to the RSEM
221 (Li and Dewey, 2011) and DESEQ (Anders and Huber, 2010) pipelines, originally used by
222 Novogene (Supplementary Information).

223 DE isoforms were detected using False Discovery Rate (FDR) adjusted p-values (named
224 hereby “q-values”), setting the threshold at 0.05. As plants responded better to metal halide
225 light, such condition was considered as control. Thus, DE genes are expressed in terms of
226 being up- or down-regulated under fluorescent light.

227 We used the DE genes calculated with Morex CDS reference for describing the patterns of
228 expression of individual genes. To reduce the number of DE genes to a workable number
229 and increase confidence, we only focused on DE genes with q-value < 0.01 (“Key genes”)
230 for producing Venn diagrams and the identification of individual genes affected by light
231 quality. All the key genes were referenced to the barley reference genomes Morex v1
232 (Mascher *et al.*, 2017), and Morex v2 (Monat *et al.*, 2019).

233 GO enrichment analysis

234 We used DE genes (q-value < 0.05) calculated from the “Tibetan transcripts” and “*de novo*
235 assembly” references in three within genotype comparisons for the GO enrichment tests.
236 We mapped the three sets of DE genes calculated from both references against the Morex
237 genome assembly WGS (Mayer *et al.*, 2012) in PlantRegMap (Jin *et al.*, 2017), which uses
238 reciprocal best BLAST hits to assign Morex gene *ids* to query sequences. Matched genes
239 received the GO terms from the Morex reference. Enrichment analysis was calculated by
240 Fisher’s exact test, with the complete gene set of Morex as control. GO terms with a q-
241 value < 0.05 were considered enriched. GO term enrichment analysis was performed
242 independently for the three sets of DE genes derived from the two mapping references; we
243 considered GO terms enriched in both references for each of the three within genotype
244 comparisons as highly reliable.

245 Clusters of DE genes

246 From within genotype comparisons in the two light conditions, we selected DE genes
247 obtained using the Morex CDS sequences as mapping reference. TPMs values were
248 clustered by the k-means method using the ‘eclust’ function from the ‘factoextra’ R

249 package (Kassambara and Mundt, 2020), which separates the points into a defined k
250 number of groups and returns the total within-cluster sum of squares. The optimal number
251 of clusters was calculated minimizing and stabilizing that term.

252 Motif discovery

253 We manually selected some clusters based on their different expression patterns between
254 light conditions in sensitive and insensitive varieties. To retrieve promoter sequences of the
255 corresponding clustered DE genes, we extracted upstream sequences (−500, +200
256 nucleotides around annotated Transcription Start Sites) for each gene, from the server
257 <http://plants.rsat.eu> (Nguyen *et al.*, 2018) and performed the motif discovery protocol
258 described in Contreras-Moreira *et al.* (2016) and Ksouri *et al.* (2021). For each cluster
259 analyzed, 50 clusters of the same size made by random picking upstream barley sequences
260 were used as negative controls for assessing the significance of motifs found (parameters
261 MAXSIGGO=60 MAXSIG=10 MINCOR=0.7 MINNCOR=0.5). The resulting motifs were
262 compared to motifs annotated in the footprintDB database (Sebastian and Contreras-
263 Moreira, 2014). The complete motif discovery results are available at
264 http://rsat.eead.csic.es/plants/data/light_report.

265 Results

266 Diversity in the response to different light sources

267 The three varieties differ in growth habit. The *HvVrn2* gene is present in Esterel and Price
268 and absent in WA1614-95 (Supplementary Table S1), and all three genotypes have a winter
269 allele at *HvVrn1*. Therefore, Esterel and Price are winter varieties, whereas WA1614-95 is a
270 facultative variety. The vernalization treatment placed the three lines at a similar

271 developmental stage (between Z11 and Z12) at the beginning of the light treatments. Under
272 M conditions, development was accelerated, compared to F, as revealed by the more
273 developed apices in 23-day old plants (Figure 1A). All three varieties flowered earlier in M
274 than in F. However, Esterel showed the least differences between treatments in days to the
275 appearance of the first node (DEV31, Figure 1B) and days to awns appearance (DEV49,
276 Figure 1C, and D). WA1614-95 presented the largest differences, with Price in an
277 intermediate position (Monteagudo *et al.*, 2020).

278 RNA-seq performance

279 Sampling for RNA-seq took place three days before the examination of the apices shown in
280 Figure 1. At that time, all three varieties had started the reproductive phase, or at least were
281 very close to reaching that point. Sequencing cDNA of 18 samples produced a total amount
282 of 1.92 billion paired-end reads. The joint *de novo* assembly for the three genotypes
283 contained 375,488 isoforms, from which we obtained 181,337 unigenes. We benchmarked
284 different barley references for mapping reads to transcripts (Supplementary Information).
285 As Morex is the most widely used barley reference, performs well in our reference
286 benchmarking, and has been functionality annotated by the community over the years,
287 “Morex CDS sequences” were chosen to calculate gene expression values and calling DE
288 genes (Figure 2). However, because of the incomplete GO annotation of the Morex 2017
289 genome (for instance, several GO terms involved in light stress were missing), we also
290 calculated DE genes using two of the best references according to our benchmarks
291 (Supplementary Information): our assembly (“*de novo* assembly” DE genes) and the
292 “Tibetan transcripts” (Dai *et al.*, 2018). Note that DE genes calculated from these two
293 references were only used for GO enrichment analysis.

294 We used correlation coefficients between genes, estimated counts across the three
295 biological replicates, as a sample quality control. Esterel_F2 showed lower correlation
296 coefficients with the other two biological replicates than the remaining samples
297 (Supplementary Figure S1B). Consequently, replicate Esterel_F2 was discarded from
298 downstream analyses. Additionally, it is remarkable that Price and WA1614-95 expression
299 patterns were highly correlated in M conditions, consistently for all replicates
300 (Supplementary Figure S1A), but showed lower correlation coefficients in F conditions
301 (Supplementary Figure S1B), indicating similar responses of these two genotypes to M
302 light, but variable responses when exposed to fluorescent light. Esterel (insensitive
303 genotype) showed lower expression level correlation coefficients with the other genotypes
304 in both conditions.

305 Expression analysis of key genes

306 To unravel differential responses of the three genotypes to light quality, we focused on DE
307 genes occurring within each genotype across light treatments. Price, WA1614-95, and
308 Esterel initially showed 2,869, 4,218, and 3,591 DE genes with q -value < 0.05 , listed in
309 Supplementary Datasets S3, S4, and S5. To focus on genes most likely affected by light
310 conditions, we further filtered the list considering only genes with q -value < 0.01 for
311 subsequent analysis, and denoted them as “key genes”. Key DE genes in Esterel were
312 predominantly down-regulated (in F compared to M), whereas Price showed more up-
313 regulated than down-regulated genes, and WA1614-95 showed a similar number of up- and
314 down-regulated DE genes (Figure 3).

315 The intersection of key genes for the three genotypes comprised 17 sequences (Table 1).
316 Among them, *HvBM3* (*Barley MADS-box 3*), *HvBM8*, *PPD-H1* (*PSEUDO RESPONSE*

317 *REGULATOR 7*, *HvPRR37*, Turner *et al.*, 2005), *HvFT1* (*FLOWERING LOCUS T*-like,
318 Yan *et al.*, 2006) were down-regulated under fluorescent light conditions in the three
319 genotypes, whereas *HvVRT2* (*VEGETATIVE TO REPRODUCTIVE TRANSITION 2*) and
320 *RVE7*-like (*EARLY PHYTOCHROME RESPONSIVE 1/REVEILLE7*) were up-regulated in
321 fluorescent light in the three genotypes. *RVE7*-like and *HvVRT2* were expressed at higher
322 levels in WA1614-95, whereas *HvBM3*, *HvBM8*, and *HvFT1* showed higher expression in
323 the insensitive line, Esterel (Figure 4). Two genes were annotated as *HvFT1*, aligned to
324 chromosomes 3H and 7H, with the same expression levels. As *HvFT1* is located
325 exclusively on 7H (Yan *et al.*, 2006), we believe the hit on 3H probably comes from a
326 duplication/misassembly in the Morex genome assembly v1, which contains a very large
327 number of fragmented genes (Beier *et al.*, 2017; Prade *et al.*, 2018). After referencing key
328 genes to the reference Morex v2 (Monat *et al.*, 2019), we found that *HvBM8* was also
329 duplicated (*HORVU2Hr1G063800* and *HORVU2Hr1G063810*, Supplementary Dataset
330 S1), thus leaving 15 single copy key DE genes in the three lines (Figure 3). The 15 key
331 genes were grouped in 14 high confidence (HC) and 1 low confidence (LC) genes
332 according to their annotation. Only the LC gene (*Ethylene-responsive transcription factor*)
333 followed different expression patterns among genotypes (up-regulated in F in the sensitive
334 genotypes, Price and WA1614-95 and down-regulated in the insensitive genotype Esterel).
335 This gene lacks a functional annotation in Morex v1 (only 159 bp were found in common
336 between the 2017 reference and the RNA-seq sequences). Instead, in Morex v2 the gene
337 has a larger coverage (539 bp). The remaining DE genes showed the same expression
338 directions in all three genotypes.

339 When we looked into key DE genes shared by just two varieties (Supplementary Dataset
340 S1), Price and WA1614-95 (both considered sensitive lines to light quality) had the largest
341 number (125, 66 up-regulated and 59 down-regulated in F, all in the same direction for both
342 genotypes). In the set of DE genes shared by Esterel and Price, 20 genes showed
343 differential expression with the same sign (14 up and 6 down), and 3 genes were different
344 (up-regulated in Price and down-regulated in Esterel). Among the DE gene set shared by
345 Esterel and WA1614-95, there were 13 genes with similar, and 29 with opposite trends.
346 WA1614-95 had more up- (35) than down-regulated (7) genes, whereas Esterel had more
347 down- (32) than up-regulated (10).

348 In the intersection between Price and WA1614-95, several transcripts coding for jasmonate-
349 induced proteins were commonly up-regulated in condition F. When focusing on the DE
350 genes in the intersection between WA1614-95 and Esterel, two WRKY family TFs with q
351 value<0.01 were identified (Supplementary Dataset S1). With the initial q-value threshold
352 of 0.05, naturally more genes were found (Supplementary Dataset S2), mostly up-regulated
353 in F in the sensitive genotype WA1614-95 and down-regulated in the insensitive Esterel.
354 Also, MADS-box TFs appeared frequently in the list of DE genes (as mentioned
355 previously, *HvVRN1*, *HvVRT2*, *HvBM3*, *HvBM8*, *HvBM10*, *HvOS2*). Among genes
356 annotated as MADS-box TFs, *HORVU3Hr1G095090* displayed the most extreme
357 contrasting pattern of expression between sensitive (up-regulated) and insensitive
358 (unchanged) varieties. BLASTN searches against NCBI nt and Ensembl Plants (Howe *et*
359 *al.*, 2020) databases revealed high similarity of this gene with a member of the wheat *FLC*
360 subclade (*TaFLC-A4-2*, Schilling *et al.*, 2020), and with *HvOS2* (*HORVU3Hr1G095240*), a
361 neighbor gene on chromosome 3H. The latter has similar expression patterns (see section

362 *Relevant light-response and developmental genes*), which might indicate a tandem
363 duplication of *FLC*-like genes.

364 GO enrichment analysis

365 We carried out a GO enrichment analysis to find functional commonalities among the
366 genes present in each of the three sets of within genotype DE genes through shared GO
367 terms. Within genotype DE genes calculated were independently subjected to GO
368 enrichment analysis with “*de novo* assembly” and “Tibetan transcripts” as references. For
369 robustness, the intersection of the resulting terms was declared as the final set of enriched
370 GOs for each within genotype comparison (Supplementary Dataset S6). The main
371 functional terms associated with DE genes are represented in Figure 5, with those involved
372 in responses relevant for this study summarized in Supplementary Figure S3. Overall, the
373 GO terms of DE genes suggest that major changes among varieties are related to translation
374 and diverse metabolic processes. Those terms were associated with genes up-regulated in
375 WA1614-95 and down-regulated in Price and Esterel (Figure 5A). The generic term
376 “translation” also belongs to many biological processes already represented among the
377 most significant GOs (organic substance metabolism process, cellular protein metabolic,
378 cellular macromolecule biosynthetic, amide biosynthesis process, etc.). Thus, translation
379 seems to be the main process underlying the extreme sensitivity of WA1614-95. Genes
380 annotated with this GO category (n=153), mostly up-regulated, were related to ribosomal
381 proteins in WA1614-95 (Supplementary Dataset S4), contrasting with the 37 and 121 DE
382 genes found in Price and Esterel, respectively, mostly down-regulated in fluorescent light
383 (Supplementary Datasets S3 and S5). Furthermore, the responses to light spectra seem
384 variety-specific. Down-regulated DE genes in F were specifically associated with

385 photosynthesis and responses to light stimulus and radiation in WA1614-95, to chloroplast
386 organization in Price, and to organic substances metabolism and vacuolar activity in Esterel
387 (Figures 5A and 5B).

388 We then relaxed the selection criteria of GO enrichment (p -value < 0.05), to have a wider
389 look at categories involving developmental and light-specific responses (Supplementary
390 Figure S3). Photosynthesis and responses to radiation, and abiotic stimulus, among others,
391 were up-regulated in F in the insensitive genotype and down-regulated in the sensitive
392 genotypes. Responses to starvation (down-regulated in F) and reproductive development
393 (up-regulated in F) were only enriched in Esterel, whereas the response to red or far-red
394 light appeared solely up-regulated in F in Price, and responses to UV-A and oxidation, and
395 photosynthesis GOs appeared exclusively in WA1614-95 (down-regulated in F).

396 Clusters of DE genes

397 To determine genes with possible common regulation, the Morex CDS DE genes (q -
398 value < 0.05), were grouped based on their expression patterns (see Figure 2). We created
399 three sets of clusters, one for each of the three ‘within genotype’ DE gene sets. The optimal
400 number of clusters was 39 for Price, 30 for Esterel, and 37 for WA1614-95. The clusters
401 revealed different patterns of expression (Figure 6). Among them, some grouped genes with
402 marked downregulation in F exclusively in the most sensitive variety WA1614-95 (Figure
403 6A, 6B). Other clusters grouped genes up-regulated in F in the sensitive varieties while
404 showing stable expression in the insensitive (Figure 6C and 6D).

405 Cluster 16 from the Price DE genes showed a common up-regulation in F in the three
406 varieties (Figure 6E). The 5 clusters highlighted (Clusters 10, 33, 36, 37 in WA1614-95 and

407 Cluster 16 in Price) were subjected to a motif discovery analysis. Upstream sequences of
408 genes within clusters 16 and 33 showed enriched DNA conserved motifs similar to
409 *Arabidopsis* ANAC092 (Figure 6F), suggesting that a barley homolog of ANAC092 could
410 be coordinating the expression of the genes within these clusters.

411 Relevant light-response and developmental genes

412 A large number of DE genes were found (Supplementary Datasets S3, S4, and S5) beyond
413 those in Table 1. We narrowed down the list focusing on genes known to be involved in
414 light perception (phytochromes, cryptochromes), circadian clock, flowering initiation, and
415 development (Figure 7). Among these, we found that *HvPhyC* was up-regulated in F in the
416 three genotypes, whereas *HvPhyB* and *HvCry2* were only differentially expressed in Price
417 (up-regulated in M), whilst no differences were found for *HvPhyA* or *HvCry1a*
418 (Supplementary Figure S2). Two TFs that act downstream in the photoreception machinery
419 and the light-signal transduction, *HvPIF5*, and *HvHY5*, were expressed with the same
420 pattern as *HvPhyC*.

421 The three genotypes showed reduced transcription levels of *PPD-H1*, *HvFT1* (Figure 4),
422 and *HvVRN1* (Figure 7) in fluorescent conditions, consistent with the delayed plant
423 development. Esterel showed higher expression levels than the sensitive genotypes for
424 *HvFT1* and *HvVRN1*, in accordance with its accelerated development in both conditions.
425 Besides, the three genotypes showed increased transcript levels of the flowering repressors
426 *HvOS2* (Figure 7), *HvVRT2*, and an orthologue of *RVE7*-like in wheat under fluorescent
427 light (Figure 4). WA1614-95, which was the latest flowering genotype, showed the highest
428 transcript levels of these repressor genes. On the other hand, *HvFPF1*-like (*Flowering*
429 *Promoting Factor 1*) transcripts were up-regulated in Price and WA1614-95 under M.

430 We also identified some differentially expressed genes, mainly in Price and some of them
431 in WA1614-95, that encode components of the circadian clock: *HvCCA1*, *HvLUX*, and
432 *HvPRR73* up-regulated in F; *HvGI*, *HvTOC1*, and *HvPRR95*, down-regulated in F; and
433 clock output genes, as *HvCO1*, up-regulated in F.

434 Two members of the *C-REPEAT/DREB BINDING FACTOR* (CBF) family (*HvCBF14*,
435 *HvCBF4a*), one member of the *COLD-RESPONSIVE* (COR) family (*WCOR15A*) and one
436 from the *INDUCER of CBF EXPRESSION* (*ICE*), an ortholog of rice (*ICE-like* annotated as
437 *metacaspase D*), all relevant in the acquisition of freezing tolerance, were up-regulated in
438 fluorescent light, mainly in the sensitive genotypes (Figure 8).

439 The RNA-seq results were validated through qRT-PCR analysis using 10 genes responsive
440 and non-responsive to light quality conditions (Figure 9). Samples were extracted from the
441 same genotypes, conditions, and age in an independent experiment. We obtained a positive
442 Pearson correlation ($r = 0.70$).

443 **Discussion**

444 Light quality affects to development genes

445 Delayed development of fluorescent light-grown plants was paralleled by dramatic changes
446 in the expression of development-related genes, which were overrepresented among the
447 14+1 key DE genes. Among them, the flowering repressors *RVE7-like*, *VRT2*, and *ICE-like*
448 were up-regulated in fluorescent light, whereas *API* MADS-box photoperiod responsive
449 genes *HvBM3* and *HvBM8*, and *HvFT1* were down-regulated. The large reduction of
450 expression of *PPD-H1* could explain the downregulation on these last three genes because
451 it mediates the long-day induction of *HvFT1* (Turner *et al.*, 2005), and several studies have

452 reported the *PPDH1*-dependent up-regulation of *HvBM3* and, *HvBM8* during development
453 (Digel *et al.*, 2015, 2016; Ejaz and von Korff, 2017).

454 GO analysis of DE genes did not suggest the existence of general responses to light spectra.
455 Differences in overrepresented GO terms among the three varieties indicated the presence
456 of different light quality responses. For instance, translation and diverse metabolic
457 processes were associated with up-regulated genes in the sensitive-extreme variety and
458 down-regulated in the other two (Figure 5A). Ribosomal protein genes were
459 overrepresented in the sensitive-extreme variety, indicating a transcriptional
460 reprogramming or translational regulation only in this genotype, as found in other species
461 subjected to biotic and abiotic stresses (Solano-De la Cruz *et al.*, 2019). Furthermore, genes
462 down-regulated in F were associated with chloroplast and plastid organization and
463 photosynthesis responses in the sensitive varieties only, and not in Esterel (Figure 5;
464 Supplementary Figure S3). Therefore, the fluorescent light spectrum might alter the
465 photosynthetic electron transport chain differently in these barley varieties. In conclusion,
466 the different grades of sensitivity to light spectra were associated with transcriptional
467 reprogramming, plastid signals, and photosynthesis. Interestingly, plant development
468 reprogramming in response to high light intensity in *Arabidopsis thaliana* has been related
469 to epigenetic changes involving *FLC* activity (Feng *et al.*, 2016). Fittingly, *HvOS2*, the
470 barley *FLC* orthologous gene, was up-regulated in F in both sensitive varieties.

471 Sensitive varieties experienced partial reversion of vernalization and
472 displayed cold tolerance responses

473 Sensitive and insensitive varieties showed strikingly different patterns of DE genes.
474 However, there was a remarkable similarity in the sets of DE genes for sensitive varieties
475 WA1614-95 and Price.

476 TFs seemed overrepresented among the DE genes. Although some MADS-box TFs were
477 equally affected across varieties (*HvBM3*, *HvBM8*, *HvVRT2*), other MADS-box genes
478 showed contrasting patterns following the varieties' sensitivity. This was the case of *FLC*-
479 like *HvOS2* and its paralog *HORVU3Hr1G095090*. In wheat, the duplication within the
480 *FLC*-clade has been related to adaptation (Schilling *et al.*, 2020). *HvOS2* represses the
481 expression of *Flowering Promoting Factor1*-like genes (Greenup *et al.* 2010; Hemming *et*
482 *al.* 2012), which also appear differentially expressed in our study (Figure 7). *HvOS2*
483 expression responds to cold, mediated by *HvVRN1*, which was also differentially expressed
484 only in the sensitive varieties. This gene should have been fully induced after vernalization
485 in all three varieties (even more so in WA1614-95, which needs little vernalization), but it
486 was less induced in F light in Price and WA1614-95, not different from a light-mediated
487 de-vernalization.

488 The high expression of *HvOS2* and its nearby paralog, as well as other genes related to cold
489 acclimation (*HvCBF14* and *WCOR15a*) under F light in sensitive varieties, bodes well with
490 their reduced *HvVRN1* expression because all these genes are VRN1 targets in barley
491 (Deng *et al.*, 2015). Cold-acclimation responses elicited by light are not a new finding.
492 Novák *et al.* (2016) reported that barley plants grown under fluorescent light supplemented

493 with far-red light presented high *HvCBF14* induction, increasing their freezing tolerance,
494 but these results were found in plants during the hardening process, not in fully vernalized
495 plants grown under inductive conditions, as was the case here. We also found two members
496 of the CBF-clade (*HvCBF14* and *HvCBF4a*, Skinner *et al.*, 2005) up-regulated in
497 fluorescent conditions. A relationship between regulation of the *CBF* regulon and light (low
498 R:FR ratio), mediated through phytochromes, and under higher temperatures than those that
499 confer cold acclimation, was reported by Franklin and Whitelam (2007). In a related
500 manner, freezing tolerance genes were affected in *phyB*-null mutants in wheat (Pearce *et*
501 *al.*, 2016), rice (He *et al.*, 2016), and *Arabidopsis* (Franklin and Whitelam, 2007), causing
502 downregulation of a member of the *INDUCER of CBF EXPRESSION (ICE)* gene family
503 (Badawi *et al.*, 2008). All these pieces of evidence strongly suggest a role of *PhyB* in light-
504 mediated activation of cold acclimation pathway, and our results support this hypothesis.

505 Adding to the cold-like effect of the fluorescent light, genes related with cold acclimation
506 as *VRT2* (Kane *et al.*, 2005), a homolog of *RVE-7*, and an *ICE*-like protease showed
507 consistent higher expression under fluorescent light. We hypothesize that upregulation of
508 repressors and cold-induced genes under fluorescent light in fully-vernalized plants and LD
509 indicate that these plants are not sensing the favorable conditions, and remain in the cold
510 acclimation phase, eliciting cold-related responses, particularly in the sensitive varieties.

511 Sensitive varieties experienced phenomena related to senescence

512 Among the highly significant DE genes, the only one showing opposite directions between
513 insensitive Esterel (down) and the sensitive varieties (up) was an *ethylene-responsive*
514 *transcription factor*. Genes encoding for jasmonate-induced proteins were up-regulated in
515 fluorescent light in the sensitive varieties. Jasmonate and ethylene are hormones involved

516 in plants' responses to a wide range of abiotic stresses, and the latter is also involved in
517 senescence. This might be connected with *hemoglobin 1*, a key gene up-regulated under
518 fluorescent light in the three varieties. Non-symbiotic hemoglobins are involved in abiotic
519 stress responses, with a purported role in protecting cells from dehydration by modulating
520 nitric oxide concentration (Rubio *et al.*, 2019; Becana *et al.*, 2020). Sensitive varieties were
521 suffering from abiotic stress under fluorescent light, and these pathways are good
522 candidates to explain the phenotypic reactions of sensitive and insensitive varieties.

523 The clusters of DE genes up-regulated in fluorescent light in sensitive varieties were
524 enriched in regulatory motifs similar to *ANAC092*, a regulator of senescence, belonging to
525 the *NAC* family (Balazadeh *et al.*, 2010). *NAC* TFs control multiple processes, although
526 they are mainly associated with senescence and response to abiotic stresses, integrating also
527 cold signals and flowering (Yoo *et al.*, 2007). The set of DE genes shared by WA1614-95
528 and Esterel showed mostly opposite trends of expression, in accordance with their
529 sensitivities. Among them, there were several encoding for *WRKY* TF. These TFs are
530 involved in the regulation of transcriptional reprogramming associated with plant abiotic
531 and biotic stress responses (Bakshi and Oelmüller, 2014) and, at least in grapevine, *WRKY*
532 TFs trigger cell wall modifications to block the entrance of UV light into the cell
533 (Lesniewska *et al.*, 2004).

534 Interestingly, a link between cold acclimation, senescence, and flowering delay was
535 described by Wingler (2011) for *Arabidopsis thaliana* and barley. Through a promoter
536 motif analysis, this author found that flowering and senescence regulation are closely
537 associated with light and stress signaling and that cold-responsive genes were induced in
538 plants with delayed senescence.

539 Signaling pathways affected by light quality

540 The variability of expression patterns found for genes related to response to light and
541 specific spectra regions (red, far-red, UV) indicates that the treatments affected the function
542 of light receptors and photomorphogenesis. We found higher expression levels of *HvPhyC*
543 under fluorescent light in all three genotypes, and an opposite trend for *HvPhyB* and
544 *HvCry2* (consistent with their antagonist role, reported by Más *et al.*, 2000). According to
545 our results, the fluorescent light caused a strong imbalance of the expression of these three
546 signaling genes, which could lead to a disruption of 1) the balance of active and inactive
547 forms of phytochromes, 2) patterns of occurrence of homo- and heterodimers, and 3)
548 phytochromes to cryptochromes ratios. These imbalances could be at the top of the cascade
549 of changes in gene expression found in downstream pathways.

550 Both PhyC and PhyB are required for the photoperiodic induction of flowering in wheat
551 (Pearce *et al.*, 2016; Kippes *et al.*, 2020). Null wheat mutants of either *PhyC* or *PhyB*
552 produced late-flowering plants, with altered vegetative development. Up-regulation of
553 *HvPhyC* in F light resembled the phenotype of lacking a functional gene in wheat.

554 PhyC signal may have cascaded down through PPD-H1, as it is known to activate PPD-1 in
555 LD (Nishida *et al.*, 2013; Chen *et al.*, 2014; Woods *et al.*, 2014). In our study, there were
556 opposite patterns of expression between the DE genes *HvPhyC* and *PPD-H1* in the three
557 genotypes, supporting their close relation. The altered phytochrome expressions may have
558 shifted their proportions from the optimum, reducing *PPD-H1* induction in fluorescent
559 light.

560 Also, several signaling and clock genes were DE in the sensitive lines. In *A. thaliana*,
561 Franklin and Whitelam (2007) observed that the phytochrome signaling was mediated by
562 the circadian clock. Thus, the complex relation between photoreceptors and the clock might
563 provide a reason for the differences in downstream development genes, and in the
564 phenotype. It is remarkable that *HvPhyB*, *HvCry2*, and most of the clock genes represented,
565 were only differentially expressed in cultivar Price.

566 Why would an annual crop develop mechanisms of adaption to light quality?

567 We have revealed the presence of phenotypic variation of barley in response to light
568 quality. Could this variation be adaptive? Barley spread from its cradle at 35°-40°N to
569 latitudes beyond 60°N involving well-known adaptation mechanisms like insensitivity to
570 day length (Jones *et al.*, 2008). Adaptations to other possible light-related factors for crop
571 species have been largely overlooked. If factors other than day length underlie light
572 adaptation of crops, this area deserves urgent attention. Climate change is already causing
573 latitudinal shifts of variety distribution and plant breeders should know how to cope with
574 possible light-related genetic effects other than photoperiodic response (Hunt *et al.*, 2019).

575 Light quality effects have received more attention in perennials. In a recent report, Chiang
576 *et al.* (2019) found that light quality affects tree growth showing a wide natural variation.
577 This is caused by the latitudinal change in the duration of periods under low solar angles
578 and by variation of overcast conditions (that implies variable R:FR ratios). They suggested
579 that trees that originated at high latitudes are more sensitive to light quality, compared to
580 those from lower latitudes. The barley lines tested in our experiment are autumn sown, and
581 much of their growth period occurs in winter, the period of the lowest solar angle. It is
582 conceivable that annual crops also took advantage of mutations to optimize their growth in

583 regions with light quality features different from the ones found at their center of origin. In
584 addition, the solar angle in early spring is still relatively low and shows a large latitudinal
585 variation. This may have resulted in the evolvement of additional regulation mechanisms of
586 plant development at the higher latitudes, preventing the precocious initiation of stem
587 elongation in fully vernalized plants.

588 To conclude, we have found considerable variability among barley genotypes regarding
589 light quality sensitivity, involving different molecular mechanisms, akin to other abiotic
590 stress responses. Further research is needed to pin down their molecular bases and, in
591 particular, the extent of their role under natural conditions, with possible repercussions on
592 crop breeding.

593 **Supplementary data**

594 **Supplementary Tables and Figures**

595 **Supplementary Table S1.** List of the barley genotypes examined and allelic variants for
596 the major genes of flowering time.

597 **Supplementary Table S2.** Primer sequences for qRT-PCR assay.

598 **Supplementary Figure S1.** Correlation of transcript abundances across biological
599 replicates.

600 **Supplementary Figure S2.** Selection of flowering related genes (photoreceptors, circadian
601 clock and development).

602 **Supplementary Figure S3.** Enriched GO terms relevant for plant responses to light quality
603 conditions.

604 **Supplementary Information.**

605 **Supplementary Information S1.** Summary of the DE experimental design and results of
606 DE genes from within line comparison.

607 **Supplementary Information S2.** Number of differentially expressed genes (DE) in each
608 of the six between line comparisons.

609 **Supplementary Information S3.** Number of biological samples correctly clustered in the
610 hierarchical clustering generated for the nine comparisons.

611 **Supplementary Dataset.**

612 **Supplementary Dataset S1.** List of Key DE genes (q-value < 0.01) shared between
613 varieties.

614 **Supplementary Dataset S2.** List of DE genes (q-value < 0.05) shared between varieties.

615 **Supplementary Dataset S3.** List of DE genes in Price, comparison between M and F
616 conditions.

617 **Supplementary Dataset S4.** List of DE genes in WA1614-95, comparison between M and
618 F conditions.

619 **Supplementary Dataset S5.** List of DE genes in Esterel, comparison between M and F
620 conditions.

621 **Supplementary Dataset S6.** GO enrichment.

622 **Acknowledgments**

623 This work was supported by the Spanish Ministry of Economy and Competitiveness
624 (Projects AGL2013–48756-R, including a scholarship granted to AM, and AGL2016–
625 80967-R), and Spanish Ministry of Science and Innovation (PID2019-111621RB-I00). The
626 authors acknowledge Najla Ksouri and Francesc Montardit for their technical support.

627 **Author contributions**

628 AC, BC-M, EI, IK: Conception and design.

629 BC-M, AR-R: Methodology

630 AR-R, AM: Formal analysis, Writing - Original draft.

631 AM: Visualization

632 TK, MM, IK: Acquisition of data

633 AC, EI: Writing – Review & Editing, Project administration, Funding acquisition

634 AC, EI, BC-M: Supervision

635 **Data availability**

636 The data for this study have been deposited in the European Nucleotide Archive (ENA) at
637 EMBL-EBI under accession number PRJEB35759
638 (<https://www.ebi.ac.uk/ena/browser/view/PRJEB35759>). Additionally, motif discovery
639 analysis of selected clusters of differentially expressed genes is available at
640 rsat.eead.csic.es/plants/data/light_report/.

641

642

References

- Adams S, Allen T, Whitelam GC.** 2009. Interaction between the light quality and flowering time pathways in Arabidopsis. *Plant Journal* **60**, 257–267.
- Anders S, Huber W.** 2010. Differential expression analysis for sequence count data. *Genome Biology* **11**, R106.
- Badawi M, Reddy YV, Agharbaoui Z, Tominaga Y, Danyluk J, Sarhan F, Houde M.** 2008. Structure and Functional Analysis of Wheat *ICE* (Inducer of CBF Expression) Genes. *Plant and Cell Physiology* **49**, 1237–1249.
- Bakshi M, Oelmüller R.** 2014. WRKY transcription factors: Jack of many trades in plants. *Plant Signaling and Behavior* **9**, e27700.
- Balazadeh S, Siddiqui H, Allu AD, Matallana-Ramirez LP, Caldana C, Mehrnia M, Zanor M-I, Köhler B, Mueller-Roeber B.** 2010. A gene regulatory network controlled by the NAC transcription factor ANAC092/AtNAC2/ORE1 during salt-promoted senescence. *The Plant Journal* **62**, 250–264.
- Becana M, Yruela I, Sarath G, Catalán P, Hargrove MS.** 2020. Plant hemoglobins: a journey from unicellular green algae to vascular plants. *New Phytologist* **227**, 1618–1635.
- Beier S, Himmelbach A, Colmsee C, et al.** 2017. Construction of a map-based reference genome sequence for barley, *Hordeum vulgare* L. *Scientific Data* **4**, 170044.
- Bray NL, Pimentel H, Melsted P, Pachter L.** 2016. Near-optimal probabilistic RNA-seq quantification. *Nature Biotechnology* **34**, 525–527.
- Casal JJ.** 1993. Novel effects of phytochrome status on reproductive shoot growth in *Triticum aestivum* L. *New Phytologist* **123**, 45–51.
- Casas AM, Djemel A, Ciudad FJ, Yahiaoui S, Ponce LJ, Contreras-Moreira B, Gracia MP, Lasa JM, Igartua E.** 2011. *HvFT1* (*VrnH3*) drives latitudinal adaptation in Spanish barleys. *Theoretical and Applied Genetics* **122**, 1293–1304.
- Chen A, Li C, Hu W, Lau MY, Lin H, Rockwell NC, Martin SS, Jernstedt JA, Lagarias JC, Dubcovsky J.** 2014. PHYTOCHROME C plays a major role in the acceleration of wheat flowering under long-day photoperiod. *Proceedings of the National Academy of Sciences* **111**, 10037–10044.
- Chiang C, Olsen JE, Basler D, Bånkestad D, Hoch G.** 2019. Latitude and weather influences on sun light quality and the relationship to tree growth. *Forests* **10**, 1–12.
- Contreras-Moreira B, Castro-Mondragon JA, Rioualen C, Cantalapiedra CP, van Helden J.** 2016. RSAT::Plants: Motif Discovery Within Clusters of Upstream Sequences in Plant Genomes. In: Hehl R, ed. *Plant Synthetic Promoters: Methods and Protocols*. New York, NY: Springer New York, 279–295.
- Dai F, Wang X, Zhang XQ, Chen Z, Nevo E, Jin G, Wu D, Li C, Zhang G.** 2018. Assembly and

analysis of a qingke reference genome demonstrate its close genetic relation to modern cultivated barley. *Plant Biotechnology Journal* **16**, 760–770.

Davidson NM, Oshlack A. 2014. Corset: enabling differential gene expression analysis for de novo assembled transcriptomes. *Genome Biology* **15**, 410.

Deng W, Casao MC, Wang P, Sato K, Hayes PM, Finnegan EJ, Trevaskis B. 2015. Direct links between the vernalization response and other key traits of cereal crops. *Nature Communications* **6**, 5882.

Digel B, Pankin A, von Korff M. 2015. Global Transcriptome Profiling of Developing Leaf and Shoot Apices Reveals Distinct Genetic and Environmental Control of Floral Transition and Inflorescence Development in Barley. *The Plant Cell* **27**, 2318–2334.

Digel B, Tavakol E, Verderio G, Tondelli A, Xu X, Cattivelli L, Rossini L, von Korff M. 2016. Photoperiod-H1 (Ppd-H1) Controls Leaf Size. *Plant Physiology* **172**, 405–415.

Ejaz M, von Korff M. 2017. The genetic control of reproductive development under high ambient temperature. *Plant Physiology* **173**, 294–306.

Feng P, Guo H, Chi W, et al. 2016. Chloroplast retrograde signal regulates flowering. *Proceedings of the National Academy of Sciences* **113**, 10708–10713.

Franklin KA. 2009. Light and temperature signal crosstalk in plant development. *Current Opinion in Plant Biology* **12**, 63–68.

Franklin KA, Quail PH. 2010. Phytochrome functions in Arabidopsis development. *Journal of Experimental Botany* **61**, 11–24.

Franklin KA, Toledo-Ortiz G, Pyott DE, Halliday KJ. 2014. Interaction of light and temperature signalling. *Journal of Experimental Botany* **65**, 2859–2871.

Franklin KA, Whitelam GC. 2007. Light-quality regulation of freezing tolerance in *Arabidopsis thaliana*. *Nature Genetics* **39**, 1410–1413.

Greenup AG, Sasani S, Oliver SN, Talbot MJ, Dennis ES, Hemming MN, Trevaskis B. 2010. *ODDSOC2* Is a MADS Box Floral Repressor That Is Down-Regulated by Vernalization in Temperate Cereals. *Plant Physiology* **153**, 1062–1073.

Haas BJ, Papanicolaou A, Yassour M, et al. 2013. *De novo* transcript sequence reconstruction from RNA-Seq: reference generation and analysis with Trinity. *Nature protocols* **8**, 1494–1512.

He Y, Li Y, Cui L, Xie L, Zheng C, Zhou G, Zhou J, Xie X. 2016. Phytochrome B negatively affects cold tolerance by regulating *OsDREB1* gene expression through phytochrome interacting factor-like protein OsPIL16 in rice. *Frontiers in Plant Science* **7**, 1963.

Hemming MN, Peacock WJ, Dennis ES, Trevaskis B. 2008. Low-temperature and daylength cues are integrated to regulate *FLOWERING LOCUS T* in barley. *Plant physiology* **147**, 355–366.

Holmes MG, Smith H. 1977. The function of phytochrome in the natural environment - II. The influence of vegetation canopies on the spectral energy distribution of natural

daylight. *Photochemistry and Photobiology* **25**, 539–545.

Howe KL, Contreras-Moreira B, De Silva N, et al. 2020. Ensembl Genomes 2020-enabling non-vertebrate genomic research. *Nucleic Acids Research* **48**, D689–D695.

Hunt JR, Lilley JM, Trevaskis B, Flohr BM, Peake A, Fletcher A, Zwart AB, Gobbett D, Kirkegaard JA. 2019. Early sowing systems can boost Australian wheat yields despite recent climate change. *Nature Climate Change* **9**, 244–247.

Jin J, Tian F, Yang D-C, Meng Y-Q, Kong L, Luo J, Gao G. 2017. PlantTFDB 4.0: toward a central hub for transcription factors and regulatory interactions in plants. *Nucleic Acids Research* **45**, D1040–D1045.

Jones H, Leigh FJ, Mackay I, Bower MA, Smith LMJ, Charles MP, Jones G, Jones MK, Brown TA, Powell W. 2008. Population-Based Resequencing Reveals That the Flowering Time Adaptation of Cultivated Barley Originated East of the Fertile Crescent. *Molecular Biology and Evolution* **25**, 2211–2219.

Kane NA, Danyluk J, Tardif G, Ouellet F, Laliberté JF, Limin AE, Fowler DB, Sarhan F. 2005. *TaVRT-2*, a member of the *StMADS-11* clade of flowering repressors, is regulated by vernalization and photoperiod in wheat. *Plant Physiology* **138**, 2354–2363.

Kassambara A, Mundt F. (2020) factoextra: Extract and Visualize the Results of Multivariate Data Analyses. R package version 1.0.7. Retrieved January 20, 2021 from <https://CRAN.R-project.org/package=factoextra>

Kippes N, Vangessel C, Hamilton J, Akpinar A, Budak H, Dubcovsky J, Pearce S. 2020. Effect of *phyB* and *phyC* loss-of-function mutations on the wheat transcriptome under short and long day photoperiods. *BMC Plant Biology* **20**, 297.

Kleine T, Kindgren P, Benedict C, Hendrickson L, Strand A. 2007. Genome-Wide Gene Expression Analysis Reveals a Critical Role for CRYPTOCHROME1 in the Response of Arabidopsis to High Irradiance. *Plant Physiology* **144**, 1391–1406.

Ksouri N, Castro-Mondragón JA, Montardit-Tardà F, Van Helden J, Contreras-Moreira B, Gogorcena Y. 2021. Tuning promoter boundaries improves regulatory motif discovery in non-model plants: the peach example. *Plant Physiology* doi: [doi: 10.1093/plphys/kiaa091](https://doi.org/10.1093/plphys/kiaa091)

Leivar P, Monte E. 2014. PIFs: Systems Integrators in Plant Development. *The Plant Cell* **26**, 56–78.

Lesniewska E, Adrian M, Klinguer A, Pugin A. 2004. Cell wall modification in grapevine cells in response to UV stress investigated by atomic force microscopy. *Ultramicroscopy* **100**, 171–178.

Li B, Dewey CN. 2011. RSEM: Accurate transcript quantification from RNA-Seq data with or without a reference genome. *BMC Bioinformatics* **12**, 1–16.

Más P, Devlin PF, Panda S, Kay SA. 2000. Functional interaction of phytochrome B and cryptochrome 2. *Nature* **408**, 207–211.

Mascher M, Gundlach H, Himmelbach A, et al. 2017. A chromosome conformation

capture ordered sequence of the barley genome. *Nature* **544**, 427–433.

Mayer KFX, Waugh R, Langridge P, et al. 2012. A physical, genetic and functional sequence assembly of the barley genome. *Nature* **491**, 711–716.

Merotto Jr. A, Fischer A, Vidal R. 2009. Perspectives for using light quality as an advanced ecophysiological weed management tool. *Planta Daninha* **27**, 407–419.

Monat C, Padmarasu S, Lux T, et al. 2019. TRITEX: Chromosome-scale sequence assembly of Triticeae genomes with open-source tools. *Genome Biology* **20**, 284.

Monostori I, Heilmann M, Kocsy G, et al. 2018. LED Lighting – Modification of Growth, Metabolism, Yield and Flour Composition in Wheat by Spectral Quality and Intensity. *Frontiers in Plant Science* **9**, 605.

Monteagudo A, Kiss T, Mayer M, Casas AM, Igartua E, Karsai I. 2020. Genetic diversity in developmental responses to light spectral quality in barley (*Hordeum vulgare* L.). *BMC Plant Biology* **20**, 207.

Nguyen NTT, Contreras-Moreira B, Castro-Mondragon JA, et al. 2018. RSAT 2018: regulatory sequence analysis tools 20th anniversary. *Nucleic Acids Research* **46**, W209–W214.

Nishida H, Ishihara D, Ishii M, et al. 2013. *Phytochrome C* Is A Key Factor Controlling Long-Day Flowering in Barley. *Plant Physiology* **163**, 804–814.

Novák A, Boldizsár Á, Ádám É, Kozma-Bognár L, Majláth I, Bága M, Tóth B, Chibbar R, Galiba G. 2016. Light-quality and temperature-dependent *CBF14* gene expression modulates freezing tolerance in cereals. *Journal of Experimental Botany* **67**, 1285–1295.

Oakenfull RJ, Davis SJ. 2017. Shining a light on the Arabidopsis circadian clock. *Plant, Cell & Environment* **40**, 2571–2585.

Pankin A, Campoli C, Dong X, et al. 2014. Mapping-by-Sequencing Identifies *HvPHYTOCHROME C* as a Candidate Gene for the *early maturity 5* Locus Modulating the Circadian Clock and Photoperiodic Flowering in Barley. *Genetics* **198**, 383–396.

Pearce S, Kippes N, Chen A, Debernardi JM, Dubcovsky J. 2016. RNA-seq studies using wheat *PHYTOCHROME B* and *PHYTOCHROME C* mutants reveal shared specific functions in the regulation of flowering and shade-avoidance pathways. *BMC Plant Biology* **16**, 141.

Pedmale U V., Huang SC, Zander M, et al. 2016. Cryptochromes Interact Directly with PIFs to Control Plant Growth in Limiting Blue Light. *Cell* **164**, 233–245.

Pimentel H, Bray NL, Puente S, Melsted P, Pachter L. 2017. Differential analysis of RNA-seq incorporating quantification uncertainty. *Nature Methods* **14**, 687–690.

Prade VM, Gundlach H, Twardziok S, et al. 2018. The pseudogenes of barley. *The Plant Journal* **93**, 502–514.

R Core Team. (2020). A language and environment for statistical computing. R Foundation for Statistical Computing. Retrieved January 20, 2021 from <https://www.r-project.org/>

Rockwell NC, Su Y-S, Lagarias JC. 2006. Phytochrome structure and signaling mechanisms. *Annual Review of Plant Biology* **57**, 837–858.

Rubio MC, Calvo-Begueria L, Díaz-Mendoza M, et al. 2019. Phytoglobins in the nuclei, cytoplasm and chloroplasts modulate nitric oxide signaling and interact with abscisic acid. *The Plant Journal* **100**, 38–54.

Schilling S, Kennedy A, Pan S, Jermiin LS, Melzer R. 2020. Genome-wide analysis of MIKC-type MADS-box genes in wheat: pervasive duplications, functional conservation and putative neofunctionalization. *New Phytologist* **225**, 511–529.

Schmitz J, Franzen R, Ngyuen TH, Garcia-Maroto F, Pozzi C, Salamini F, Rohde W. 2000. Cloning, mapping and expression analysis of barley MADS-box genes. *Plant Molecular Biology* **42**, 899–913.

Sebastian A, Contreras-Moreira B. 2014. footprintDB: a database of transcription factors with annotated cis elements and binding interfaces. *Bioinformatics* **30**, 258–265.

Skinner JS, von Zitzewitz J, Szűcs P, Marquez-Cedillo L, Filichkin T, Amundsen K, Stockinger EJ, Thomashow MF, Chen THH, Hayes PM. 2005. Structural, Functional, and Phylogenetic Characterization of a Large *CBF* Gene Family in Barley. *Plant Molecular Biology* **59**, 533–551.

Smith H. 1982. Light quality, photoperiod, and plant strategy. *Annual Review of Plant Physiology* **33**, 481–518.

Solano-De la Cruz MT, Adame-García J, Gregorio-Jorge J, Jiménez-Jacinto V, Vega-Alvarado L, Iglesias-Andreu LG, Escobar-Hernández EE, Luna-Rodríguez M. 2019. Functional categorization of de novo transcriptome assembly of *Vanilla planifolia* Jacks. potentially points to a translational regulation during early stages of infection by *Fusarium oxysporum* f. sp. *vanillae*. *BMC Genomics* **20**, 826.

Szucs P, Karsai I, Von Zitzewitz J, Mészáros K, Cooper LLD, Gu YQ, Chen THH, Hayes PM, Skinner JS. 2006. Positional relationships between photoperiod response QTL and photoreceptor and vernalization genes in barley. *Theoretical and Applied Genetics* **112**, 1277–1285.

Tottman DR, Makepeace RJ, Broad H. 1979. An explanation of the decimal code for the growth stages of cereals, with illustrations. *Annals of Applied Biology* **93**, 221–234.

Trevaskis B, Bagnall DJ, Ellis MH, Peacock WJ, Dennis ES. 2003. MADS box genes control vernalization-induced flowering in cereals. *Proceedings of the National Academy of Sciences* **100**, 13099–13104.

Trevaskis B, Hemming MN, Peacock WJ, Dennis ES. 2006. *HvVRN2* responds to daylength, whereas *HvVRN1* is regulated by vernalization and developmental status. *Plant Physiology* **140**, 1397–1405.

Trevaskis B, Tadege M, Hemming MN, Peacock WJ, Dennis ES, Sheldon C. 2007. *Short Vegetative Phase-Like* MADS-Box Genes Inhibit Floral Meristem Identity in Barley. *Plant Physiology* **143**, 225–235.

Turner A, Beales J, Faure S, Dunford RP, Laurie DA. 2005. The pseudo-response regulator *Ppd-H1* provides adaptation to photoperiod in barley. *Science* **310**, 1031–1034.

Ugarte CC, Trupkin SA, Ghiglione H, Slafer G, Casal JJ. 2010. Low red/far-red ratios delay spike and stem growth in wheat. *Journal of Experimental Botany* **61**, 3151–3162.

Waddington SR, Cartwright PM, Wall PC. 1983. A quantitative Scale of Spike Initial and Pistil Development in Barley and Wheat. *Annals of Botany* **51**, 119–130.

Wei T, Simko V. 2017. R package “corrplot”: Visualization of a Correlation Matrix. R package version 0.84. Retrieved January 20, 2021 from <https://github.com/taiyun/corrplot>

Wingler A. 2011. Interactions between flowering and senescence regulation and the influence of low temperature in Arabidopsis and crop plants. *Annals of Applied Biology* **159**, 320–338.

Woods DP, Ream TS, Minevich G, Hobert O, Amasino RM. 2014. PHYTOCHROME C Is an Essential Light Receptor for Photoperiodic Flowering in the Temperate Grass, *Brachypodium distachyon*. *Genetics* **198**, 397–408.

Xie L, Zhang Y, Wang K, et al. 2019. *TaVrt2*, an SVP-like gene, cooperates with *TaVrn1* to regulate vernalization-induced flowering in wheat. *New Phytologist* doi: 10.1111/nph.16339

Yan L, Fu D, Li C, Blechl A, Tranquilli G, Bonafede M, Sanchez A, Valarik M, Yasuda S, Dubcovsky J. 2006. The wheat and barley vernalization gene *VRN3* is an orthologue of *FT*. *Proceedings of the National Academy of Sciences* **103**, 19581–19586.

Yan L, Loukoianov A, Blechl A, Tranquilli G, Ramakrishna W, SanMiguel P, Bennetzen JL, Echenique V, Dubcovsky J. 2004. The wheat *VRN2* gene is a flowering repressor down-regulated by vernalization. *Science* **303**, 1640–1644.

Yoo SY, Kim Y, Kim SY, Lee JS, Ahn JH. 2007. Control of Flowering Time and Cold Response by a NAC-Domain Protein in Arabidopsis. *PLoS ONE* **2**, e642.

Zadoks JC, Chang TT, Konzak CF. 1974. A Decimal Code for the Growth Stages of Cereals. *Weed Research* **14**, 415–421.

Tables

Table 1. List of DE genes (q-value < 0.01) shared by three barley varieties studied. We show up-regulated (u) and down-regulated (d) genes in fluorescent light for each genotype.

Target ID Morex v1.0 ^a	Target ID Morex v2.0 ^b	Description ^b	Gene	Cite	Price	WA1614-95	Estrel
HORVU0Hr1G003020.3	HORVU.MOREX.r2.2H G0105150.1	MADS box transcription factor	HvBM3	1, 2	d	d	d
HORVU2Hr1G063800.7	HORVU.MOREX.r2.2H G0129220.1	MADS box transcription factor	HvBM8	1, 2	d	d	d
HORVU2Hr1G063810.1					d	d	d
HORVU7Hr1G036130.1	HORVU.MOREX.r2.7H G0551090.1	MADS box transcription factor	HvVRT2	3, 4	u	u	u
HORVU7Hr1G083670.3	HORVU.MOREX.r2.7H G0591700.1	Cytochrome P450 family protein			u	u	u
HORVU2Hr1G013400.32	HORVU.MOREX.r2.2H G0088300.1	Pseudo-response regulator	HvPRR37 (PPD-H1)	5	d	d	d
HORVU4Hr1G090860.12	HORVU.MOREX.r2.4H G0348610.1	Metacaspase-1	cell death		u	u	u
HORVU5Hr1G071940.2	HORVU.MOREX.r2.5H G0405790.1	Glycosyltransferase			u	u	u
HORVU2Hr1G024120.10	HORVU.MOREX.r2.2H G0097130.1	Terpene synthase			d	d	d
HORVU0Hr1G038850.2	HORVU.MOREX.r2.6H G0516180.1	Protein kinase			u	u	u
HORVU3Hr1G111550.2	HORVU.MOREX.r2.3H G0270770.1	Ethylene-responsive transcription factor			u	u	d
HORVU3Hr1G021880.1	HORVU.MOREX.r2.3H G0198440.1	Glycosyltransferase	Glycosyltransferase		d	d	d
HORVU3Hr1G087100.1	HORVU.MOREX.r2.7H G0542540.1	Flowering locus T	HvFT1 (VRN-H3)	6, 7	d	d	d
HORVU7Hr1G024610.1					d	d	d
HORVU5Hr1G029260.1	HORVU.MOREX.r2.5H G0372130.1	Protein kinase family protein			d	d	d
HORVU2Hr1G104580.2	HORVU.MOREX.r2.2H G0162680.1	Homeodomain-like superfamily protein	RVE7-like		u	u	u
HORVU1Hr1G076460.3	HORVU.MOREX.r2.1H G0062670.1	Hemoglobin		8	u	u	u

^a Morex reference genome v1.0 (Mascher *et al.*, 2017)

^b Morex reference genome v2.0 (Monat *et al.*, 2019)

1, Schmitz *et al.* (2000); 2, Ejaz and von Korff (2017); 3, Kane *et al.* (2005); 4, Szucs *et al.* (2006); 5, Turner *et al.* (2005); 6, Yan *et al.* (2006); 7, Casas *et al.* (2011); 8, Becana *et al.* (2020).

Figure legends

Figure 1. Phenotypic differences between varieties.

A) Apex development in plants dissected 23 days after the end of the vernalization treatment. WD, Waddington stage. B) and C) Days to first node (DEV31) and awn appearance (DEV49), expressed in days from the end of the vernalization treatment, measured in 4 biological replicates. Vertical black lines represent the days of difference between fluorescent and metal halide light conditions. D) Plants photographed 58 days after the end of the vernalization treatment.

Figure 2. Pipeline of the RNA-seq analysis.

Because of the incomplete GO annotation of the Morex 2017 genome (several GO terms involved in light stress are missing), we also calculated DE genes using the two best references according to our benchmarking, for performing the GO enrichment analysis.

Figure 3. Differentially expressed (DE) genes in the three genotypes (q-value < 0.01).

A) Clustering of DE genes with Morex CDS sequences used as reference. Colour code: red, upregulated in fluorescent light; yellow, downregulated. Three biological replicates per variety and condition are represented, except for Esterel in fluorescent light, from which a replicate was discarded. F, fluorescent; M, metal halide. B) Venn diagram showing the intersection in the number of DE genes among genotypes. Blue and red arrows indicate the number of DE genes upregulated or down regulated in fluorescent conditions in each genotype. The intersection between the three varieties indicates the number of DE genes that are annotated as High Confidence (14) and Low Confidence (1) genes in the Morex genome v2 (Monat *et al.* 2019).

Figure 4. Expression levels of selected key genes belonging to flowering pathways, with similar expression patterns in the three genotypes.

Two asterisks of the same colour indicate that differences are significant at $q < 0.01$. Genes are separated in two groups: upregulated (left) and downregulated (right) under fluorescent conditions. Genotypes are coded as green (Esterel), red (Price) and blue (WA1614-95), in fluorescent (F) or metal halide conditions (M).

Figure 5. Enriched GO terms (q-value < 0.05), selected with different criteria.

A) 10 most significant GO terms for each set of up- and down-regulated genes, ordered by increasing q-value in *de Novo* reference. B) Relevant GO terms for plant responses to light quality conditions. In both cases, only enriched GO terms corresponding to biological process (P) were selected. X-axis represents the q-value of the GO terms when taking the “Tibetan” reference, in Esterel, Price and WA1614-95 for each comparison: upF (upregulated in fluorescent conditions) downF, (downregulated in fluorescent conditions). Dot size is proportional to the number of transcript counts annotated to that GO term in the correspondent DE list.

Figure 6. Relevant clusters of DE genes sharing expression patterns under fluorescent (F) and metal halide (M) conditions.

Each grey line corresponds to the expression value of one gene across the different lines and conditions. Red lines indicate the average expression value of the sequences. (A, B) Clusters showing expression differences across light treatments in the most sensitive variety in F (WA1614-95). (C, D) Clusters showing expression differences across light conditions in sensitive (WA1614-95 and Price) varieties. (E) Cluster of genes showing a concurrent pattern of expression across light conditions in the three varieties. The number of genes within each cluster is indicated above each plot. (F) Common motif domain overrepresented in genes belonging to clusters 33 and 16. The consensus sequence was discovered in an upstream region covering [-500, 200] bp. The significance of the motif is proportional to the height of the letters. The consensus sequences found are similar to that of *Arabidopsis thaliana* ANAC092 annotated in footprintDB.

Figure 7. Expression levels of flowering-related genes (photoreceptors, circadian clock and development) in the three genotypes.

Genes are separated in two groups: upregulated (left) and downregulated (right) under fluorescent conditions. F, fluorescent conditions; M, metal halide conditions. Genotypes coded as in Figure 4. Differences between treatments are significant at q-value < 0.05 (*) or q-value < 0.01 (**).

Figure 8. Expression levels of genes related to frost response in the three genotypes.

Genes are separated in two groups: upregulated (left) and downregulated (right) under fluorescent conditions. F, fluorescent conditions, M, metal halide conditions. Genotypes coded as in Figure 4. Differences between treatments are significant at q-value < 0.05 (*) or q-value < 0.01 (**).

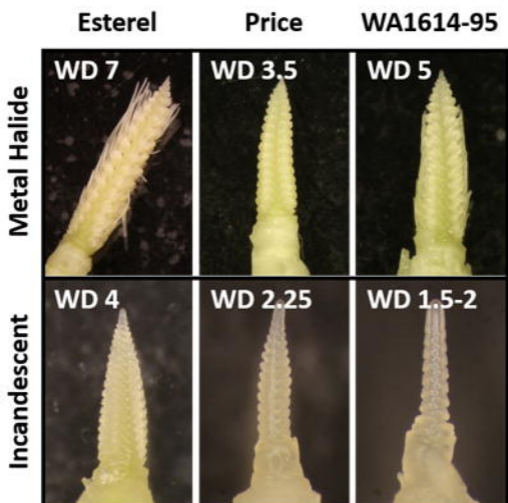
Figure 9. Correlation between RNA-seq and qRT-PCR expression values.

Values obtained after normalization (Log₂ of gene expression relative to *Actin*). The dotted line corresponds to a linear regression. R², coefficient of determination.

Figure 1

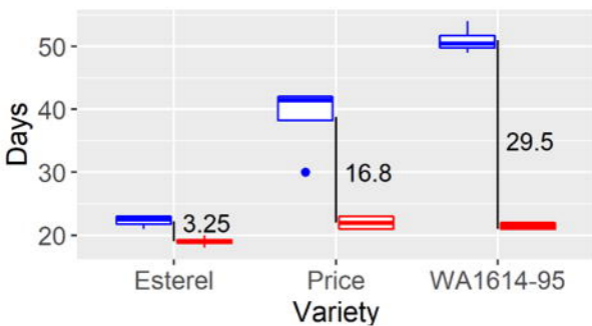
A

23 d after vernalization



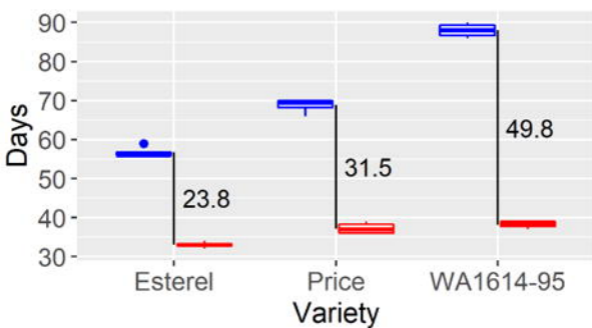
B



DEV31



C

DEV49



Condition  Fluorescent  Metal halide

D



Figure 2

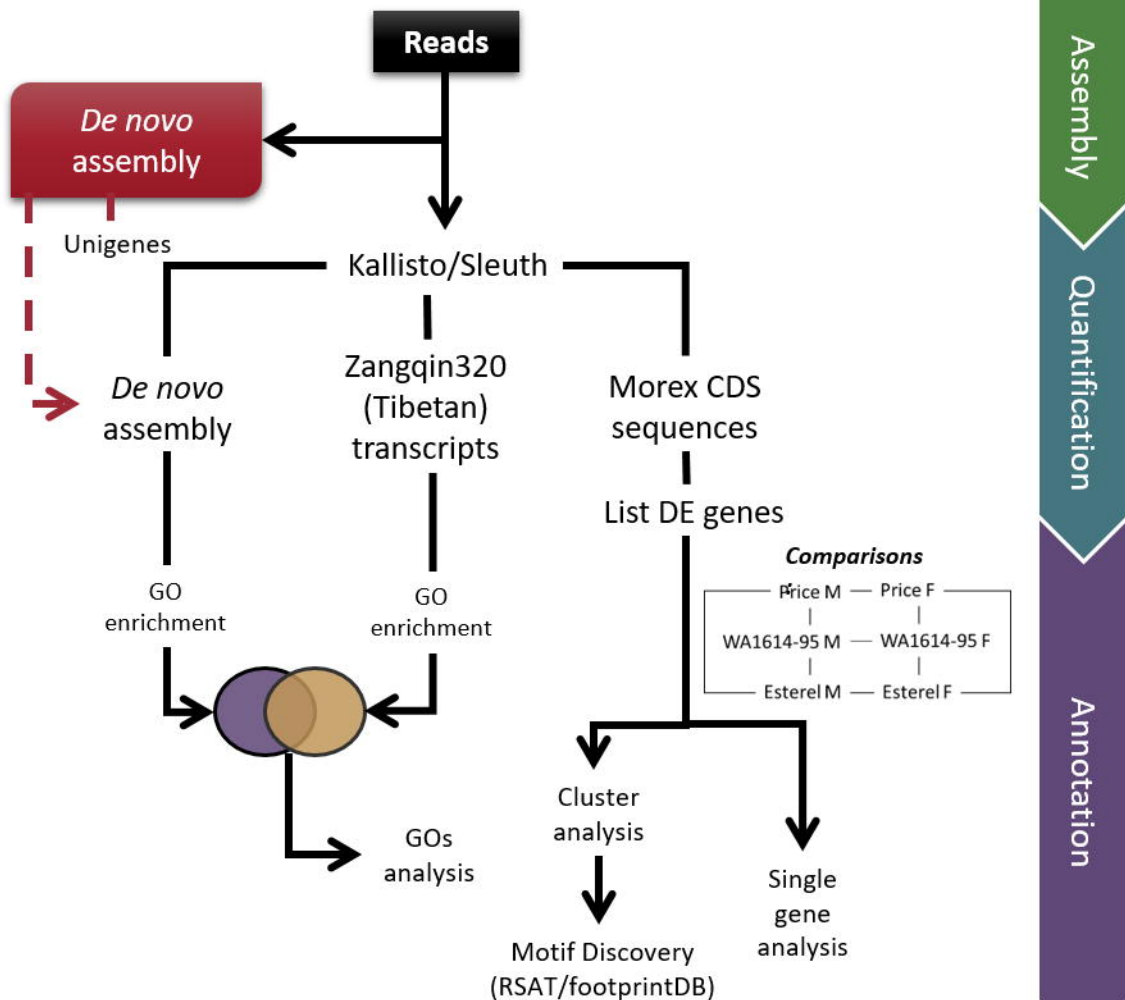


Figure 3

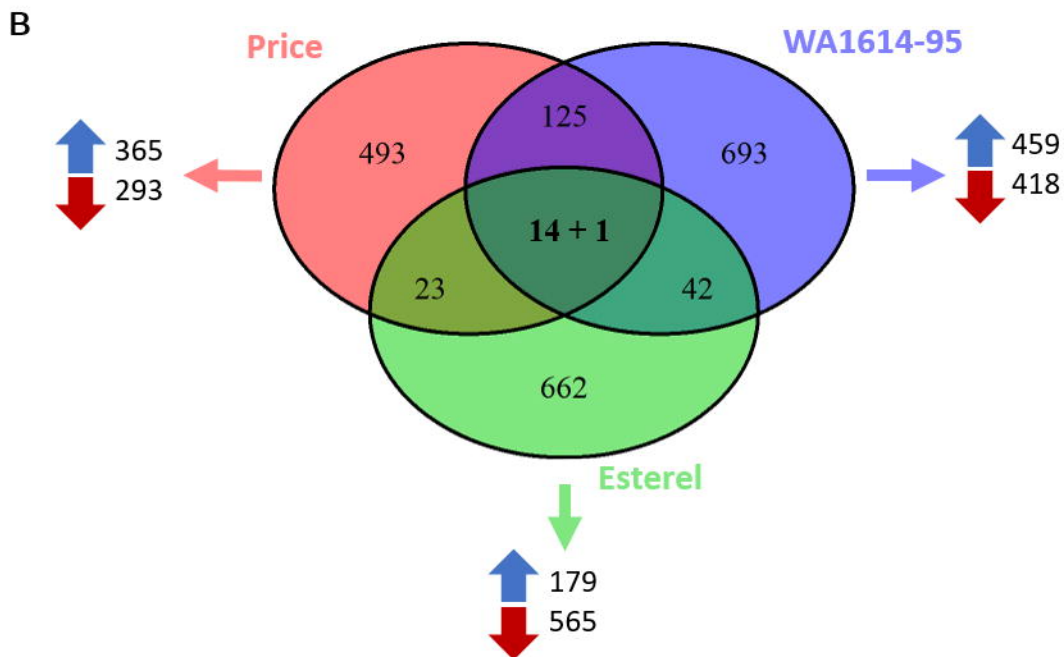
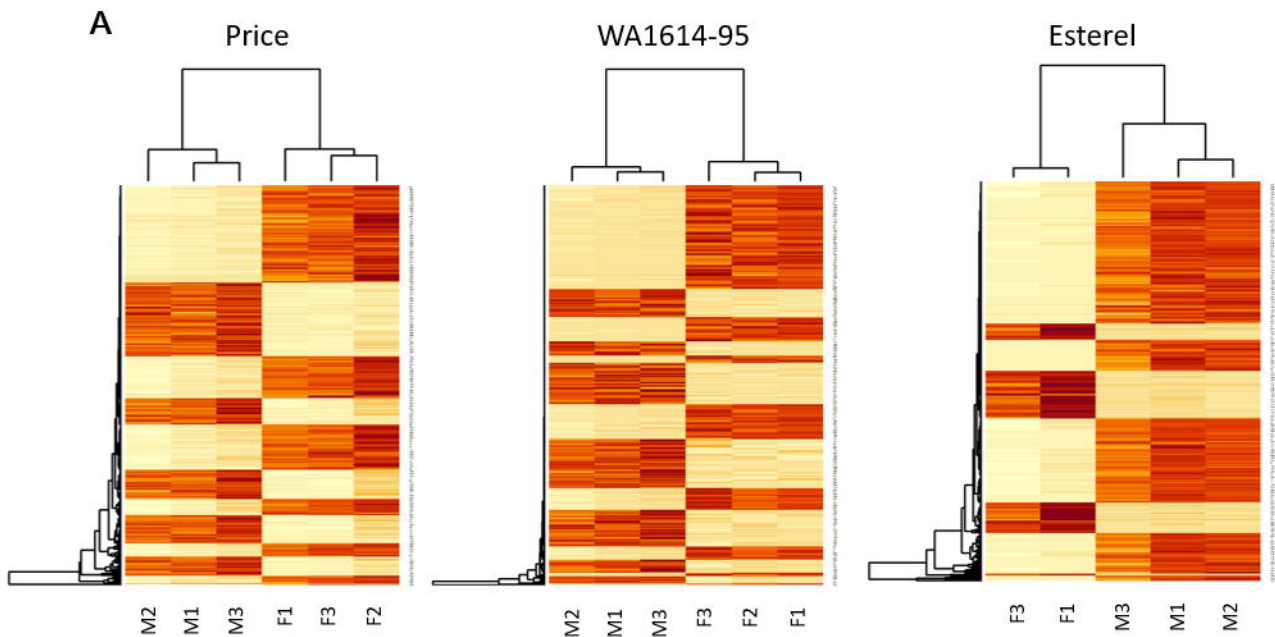
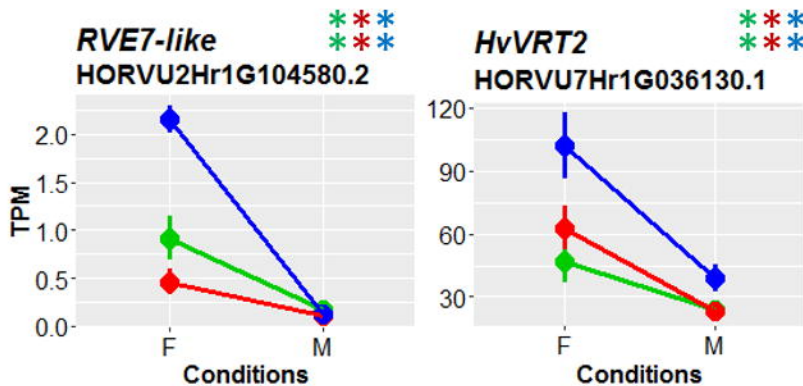


Figure 4
Upregulated in fluorescent



Downregulated in fluorescent

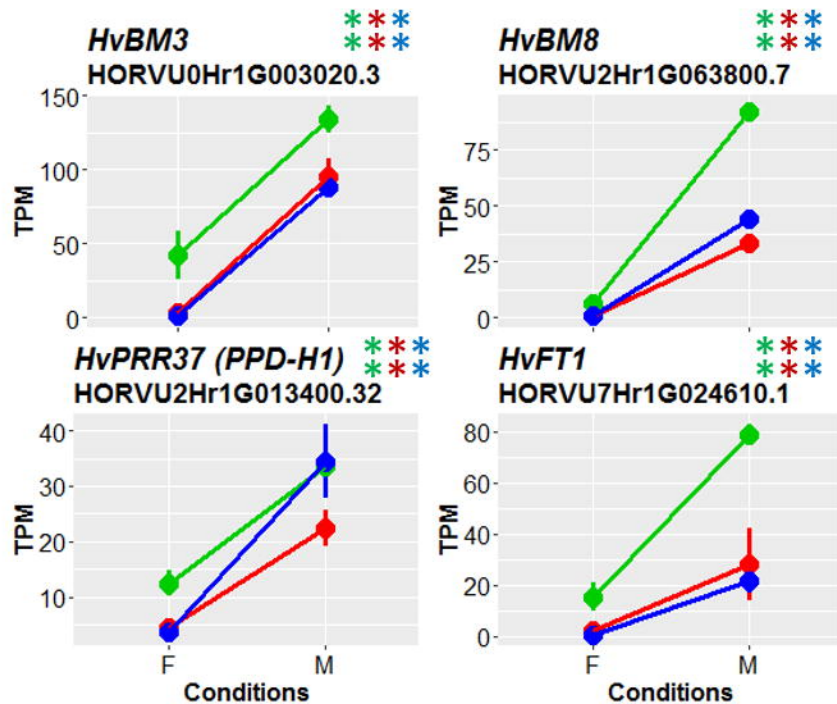
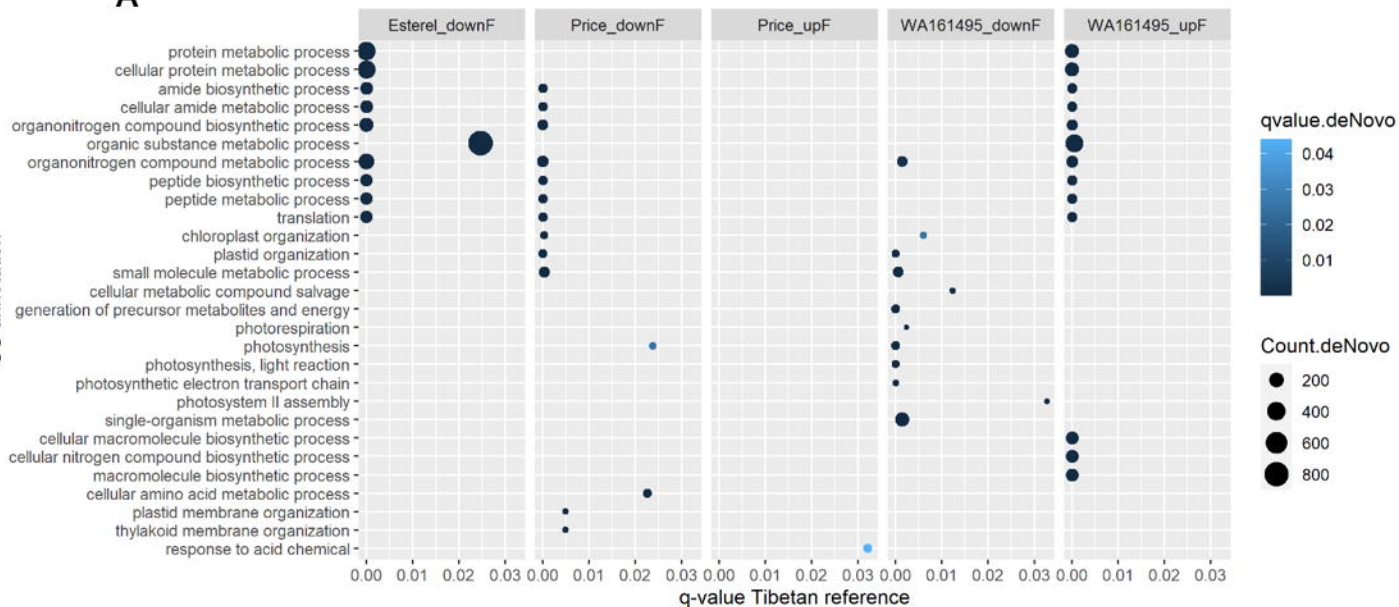


Figure 5

A



B

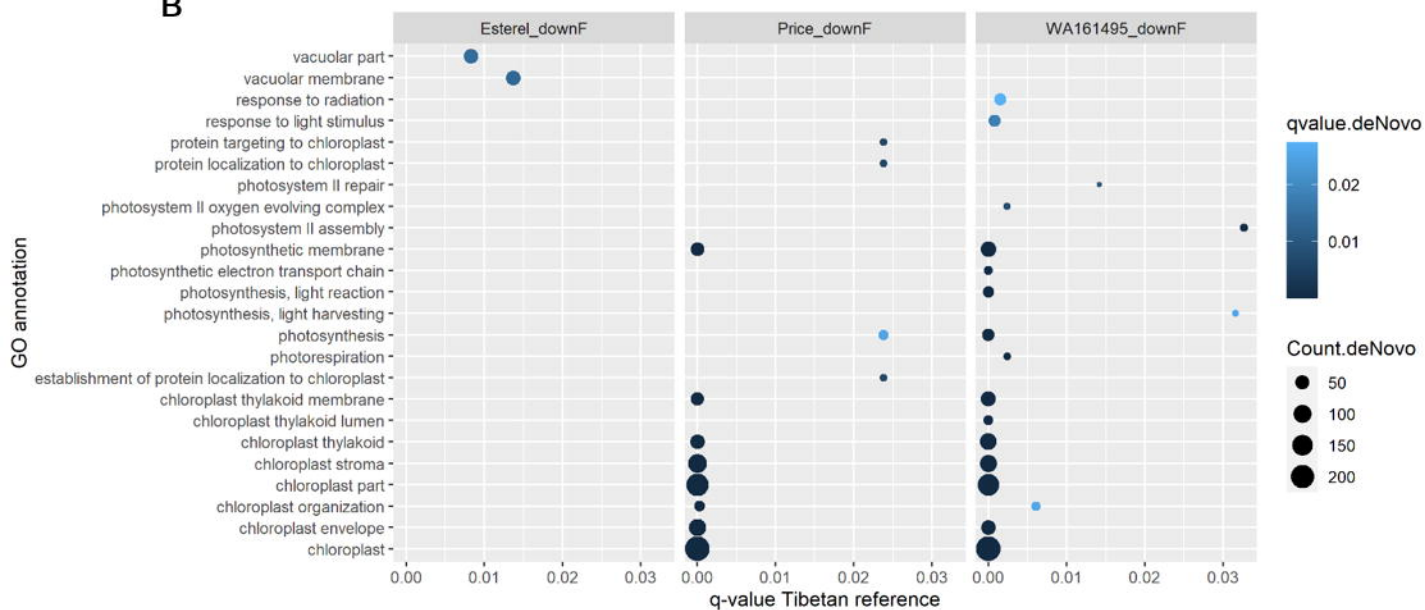


Figure 6

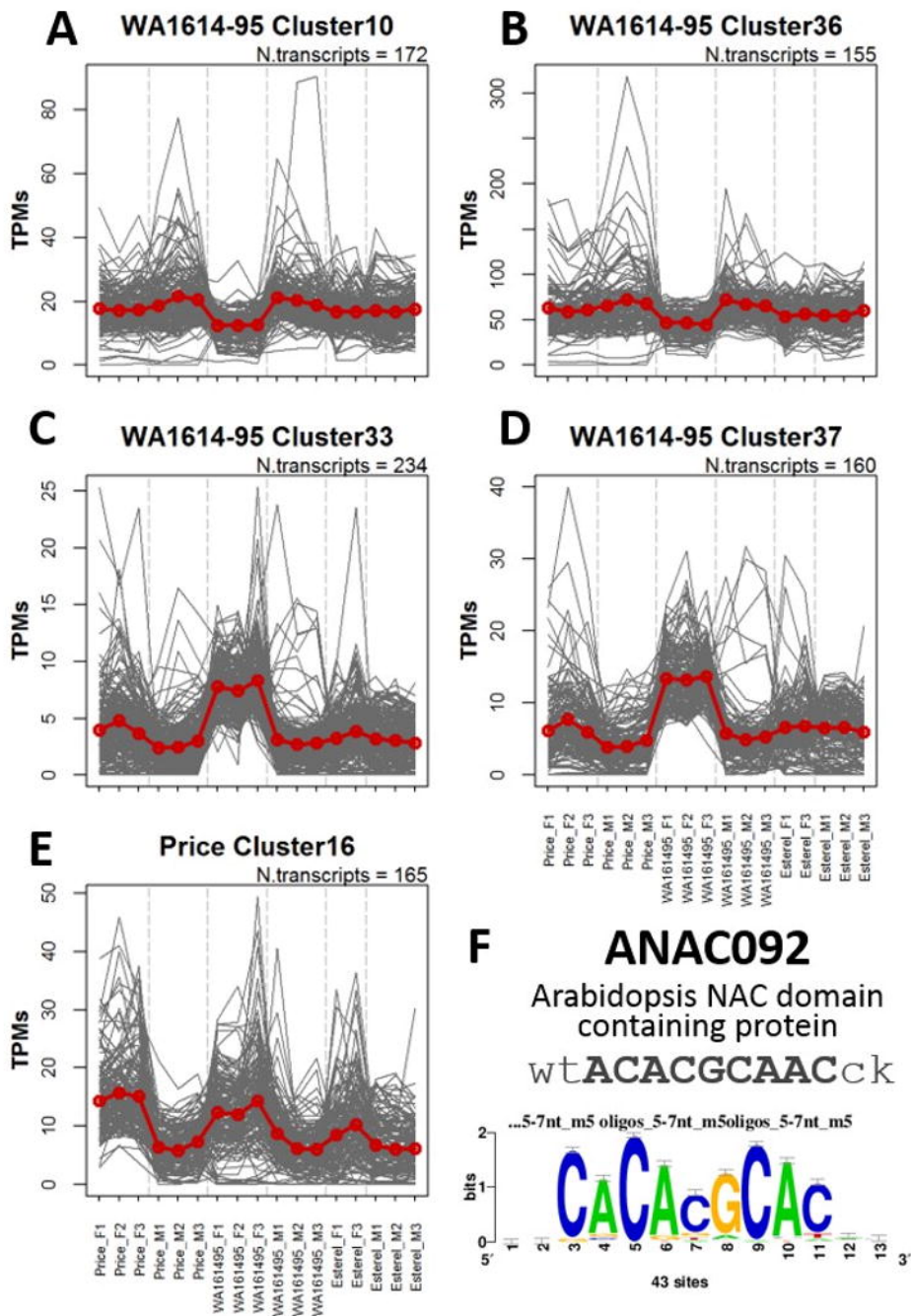
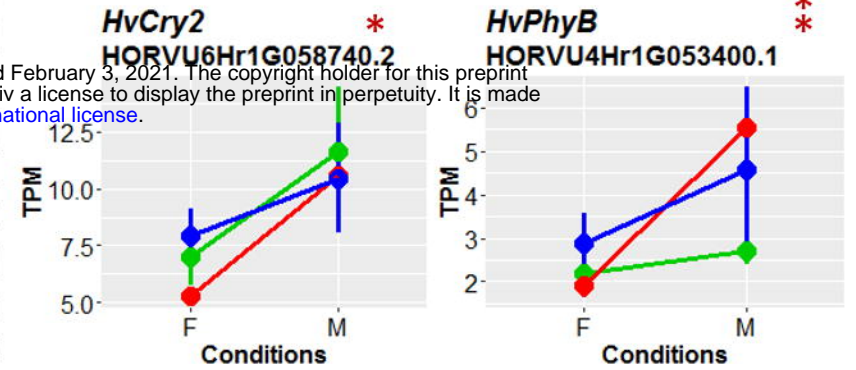
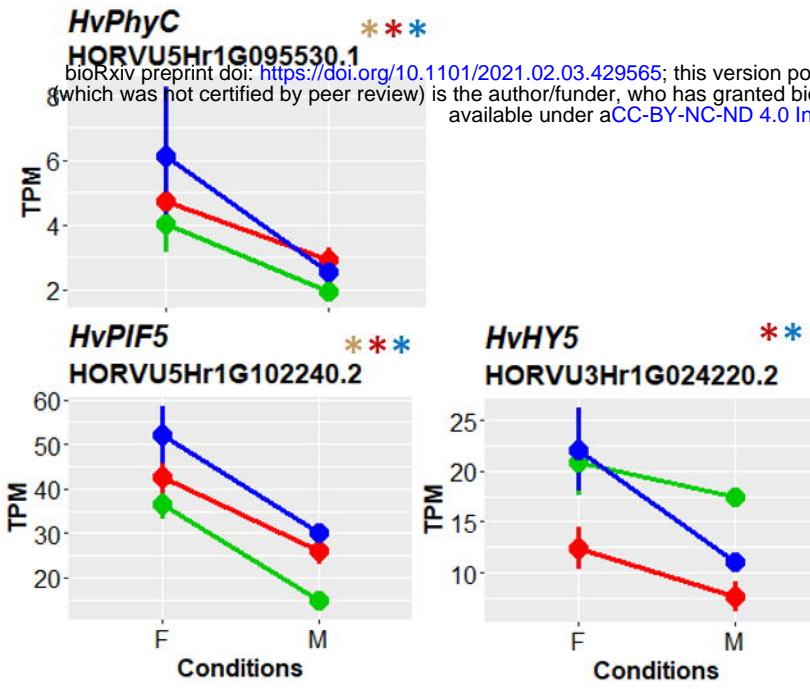


Figure 7

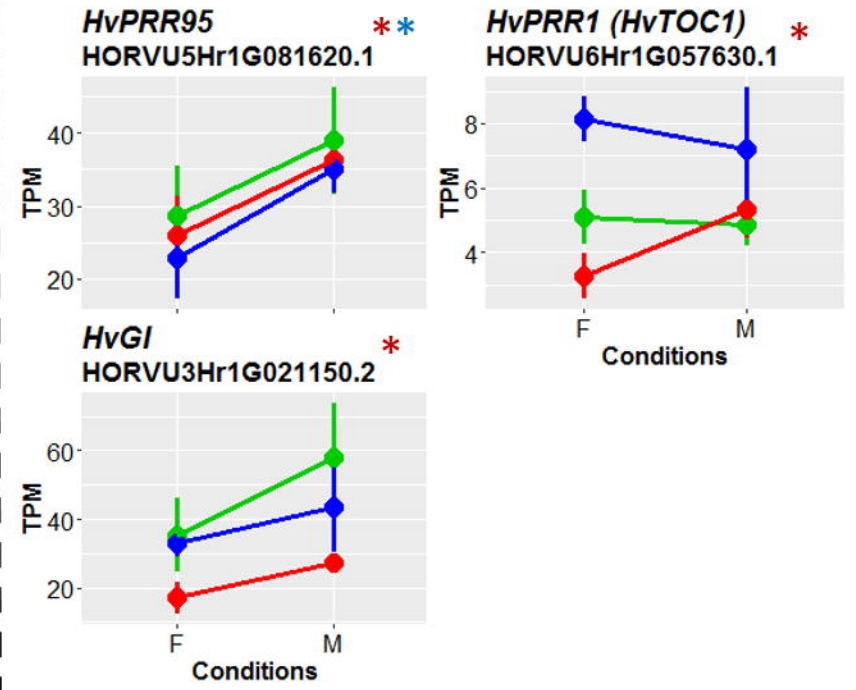
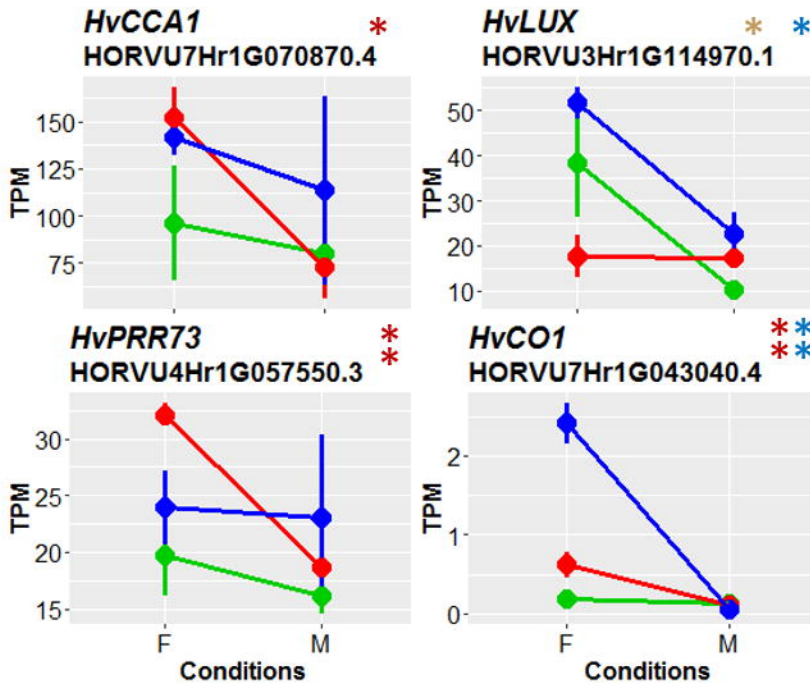
Upregulated in fluorescent

Downregulated in fluorescent

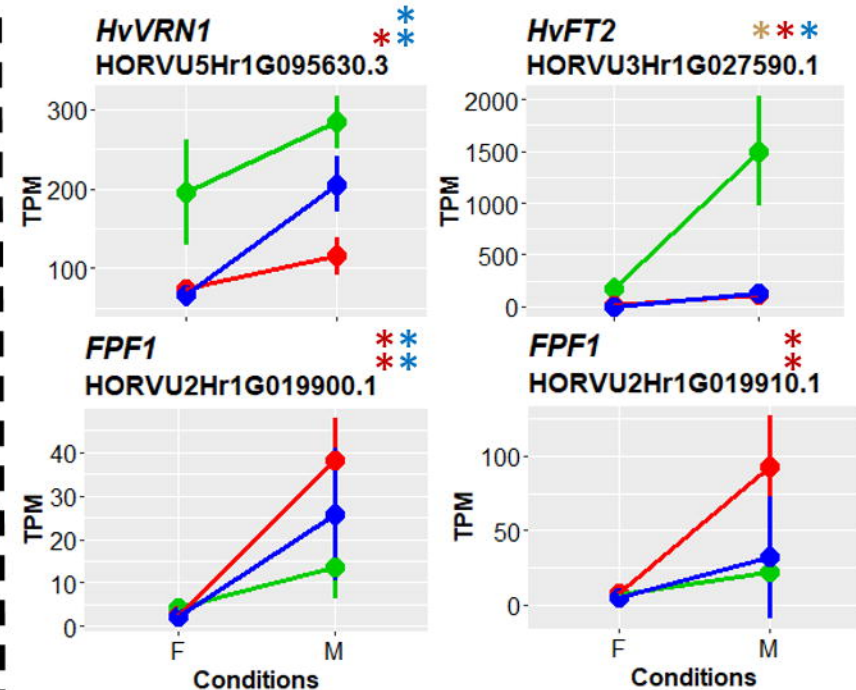
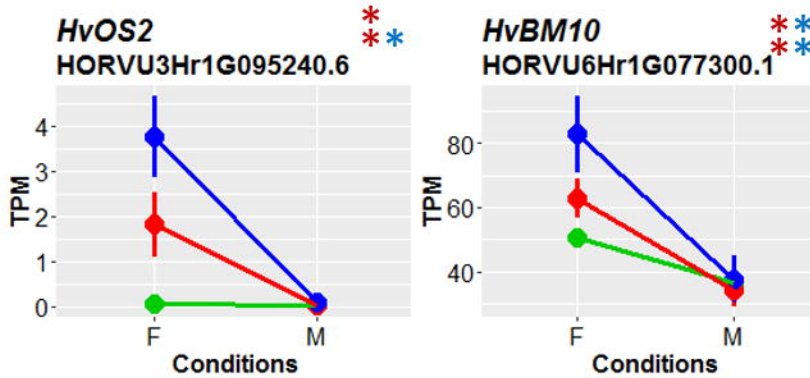
Photoreceptors



Clock



Development



Variety
 ● Esterel
 ● Price
 ● WA1614-95

bioRxiv preprint doi: <https://doi.org/10.1101/2021.02.03.429565>; this version posted February 3, 2021. The copyright holder for this preprint (which was not certified by peer review) is the author/funder, who has granted bioRxiv a license to display the preprint in perpetuity. It is made available under aCC-BY-NC-ND 4.0 International license.

Figure 8

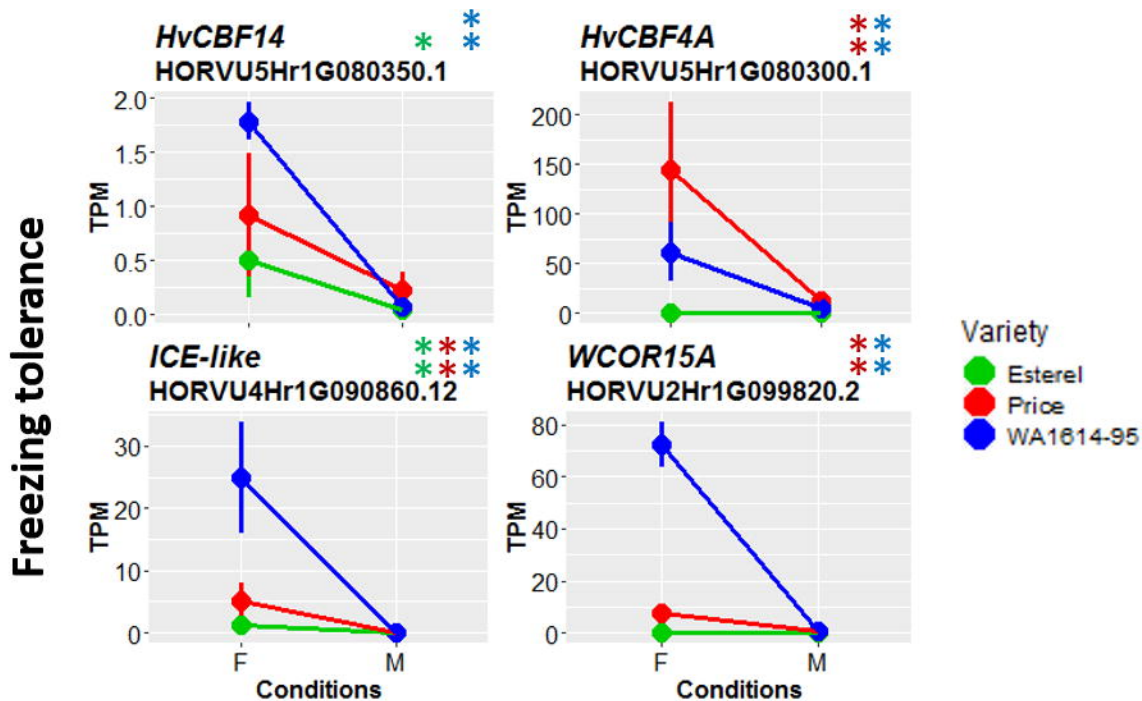


Figure 9

